



FACULTY OF TECHNOLOGY

**MODEL PREDICTIVE APPROACH FOR THE
DEMAND SIDE MANAGEMENT OF S-MARKET
TUIRA**

Janne-Pekka Nyman

Master's thesis
Degree Programme in Process Engineering
August 2020

ABSTRACT FOR THESIS

University of Oulu Faculty of Technology

Degree Programme (Bachelor's Thesis, Master's Thesis) Degree programme in Process Engineering		Major Subject (Licentiate Thesis)	
Author Janne-Pekka Nyman		Thesis Supervisor Dr.. Selek István, Prof. Ikonen Enso	
Title of Thesis Model predictive approach for the demand side management of S-Market Tuira			
Major Subject Automation Technology	Type of Thesis Master's Thesis	Submission Date November 2020	Number of Pages 77 p.
<p>Abstract</p> <p>The decrease of the ecological footprint is crucial for the continuation of modern lifestyle as it is in the future. Decarbonization of the power grid is a major step towards this goal. The renewable resources, such as solar and wind, are becoming increasingly important methods of carbon free energy production. However, their integration to the power grid faces limitations due to their inherent seasonal- and circadian rhythms. Thus, the investment into carbon free energy production is only the first part of the solution, because the intermittent nature results in curtailment phenomena, where increased renewable power generation capacity does not result in increase in renewable penetration in the power grid. To get a completely decarbonized power grid, further technical solutions are needed that enable the renewable penetration into the power grid to rise to 100 %.</p> <p>The power grid has been using top-down architecture, where the aggregator side decides the amount of power generation done by the power plants since its introduction in the beginning of 20th century. In this model, the renewable energy is a disturbance, where power generation side must accommodate to the energy demand drop that the renewable power generation causes. To fix the problem, we also must redesign the power grid infrastructure in a way that high portion of renewable energy does not endanger the power grid stability and controllability. An easier way to manage renewables is by building smart micro-grids, which is an individual power grid with two-way power transfer capabilities. This results to easier decision-making on the grid aggregator side. All the micro-grids that are connected to the main power grid can be instructed how to accommodate their energy production and management to benefit the grid stability of main power grid, and to further improve the estimation of power generation demand of conventional power plants.</p> <p>Furthermore, we must develop tools that the microgrids can utilize to balance power demand across all power grid conditions dictated by the intermittent nature of power demand and renewable energy generation. Beyond the micro-grid introduction, the renewable energy proliferation faces limitations because of the intermittent nature of the renewable energy generation. For example, increasing the capacity of solar power generation will not work to replace conventional power generation after a point if we can only utilize the generated power during daytime. The solution here is to shift the consumption from daytime to night-time. To do this, we need to consider energy storage solutions.</p> <p>This thesis explores the possibility of utilizing cooling as part of power grid management using advanced process control methods in conjunction with an Internet-of-Things approach. More specifically, I investigate the idea of using refrigeration systems as one-way energy sinks that can be used to time-shift the consumption of electricity by storing at peak renewable power generation periods. The target system of the work is the steam-compression-cooling cycle of S-Market Tuira in Oulu, which has a carbon dioxide circulation. In his 2016 Master's thesis dissertation, Jarno Johannes Tenhoma has introduced a dynamic linear time variant state model that reflects the dynamics of the cycle, thus telling about the thermal inertia of the cooled products and thus the electricity demand of the cycle. In this work, a Model Predictive Controller is derived using a dynamic model of refrigeration systems, whose function is to control the air temperatures of the store's refrigerators and freezers, which in turn are followed by the temperatures of the refrigerated products. The MPC control calculates the optimal control trajectory for the cooling system actuator, with which the temperature of the refrigeration system deviates from the set-point temperature as little as possible during the selected prediction horizon.</p> <p>Additionally, the different set-point temperature selection strategies are benchmarked in comparison to each other. The spot-price -based control changes the temperature set-point temperatures of the coolers and freezers according to Nord pool spot price data. The renewable portion data -based control strategies are based on power production data for the power grid in Finland provided by organization <i>Energiateollisuus</i>. For the purposes of testing the MPC controller and control strategy benchmarking, I have built a real-time interactive simulator in Matlab -program to illustrate the function and dynamics of the refrigeration systems of the supermarket.</p>			

TIIVISTELMÄ OPINNÄYTETYÖSTÄ

Oulun yliopisto Teknillinen tiedekunta

Koulutusohjelma (kandidaatintyö, diplomityö) Prosessitekniikan koulutusohjelma		Pääaineopintojen ala (lisensiaatintyö)	
Tekijä Janne-Pekka Nyman		Työn ohjaaja yliopistolla Dr.. Selek István, Prof. Ikonen Enso	
Työn nimi Malli-ennustava lähtökohta energia tarpeen hallintaan Tuiran S-Marketille			
Opintosuunta Automaatiotekniikka	Työn laji Diplomityö	Päiväys Joulukuu 2020	Sivumäärä 77 s.
<p>Tiivistelmä</p> <p>Ekologisen jalanjäljen laskeminen on ratkaisevaa modernin elämäntavan jatkamisen ylläpitämiseksi. Hiilipohjaisista polttoaineista luopuminen sähköverkon ylläpitämiseksi on merkittävä askel kohti tätä tavoitetta. Uusiutuvista lähteistä, kuten aurinko- ja tuulivoimasta, on tulossa yhä tärkeämpiä menetelmiä hiilivapaassa energiantuotannossa. Niiden integroimisessa sähköverkkoon on kuitenkin rajoituksia johtuen niiden tyypillisistä vuodenaika- ja vuorokausirytmiriippuvaisuuksista. Siten investointi hiilettömään energiantuotantoon on vasta ensimmäinen osa ratkaisua, koska niiden ajoittainen luonne johtaa pullonkaulailmiöön, joissa uusiutuvan sähköntuotantokapasiteetin kasvu ei enää lisää uusiutuvan energian sitoutumista sähköverkkoon. Täysin hiilettömän sähköverkon aikaan saamiseksi tarvitaan lisää teknisiä ratkaisuja, joiden avulla uusiutuvien energialähteiden tunkeutuminen sähköverkkoon voisi nousta jopa 100 prosenttiin.</p> <p>Sähköverkossa on jo 1900-luvun alusta asti käytetty ylhäältä alas -arkkitehtuuria, jossa aggregaattipuoli päättää voimalaitosten tuottaman sähkön määrän. Tässä mallissa uusiutuvan energian tuotanto on 'häiriötekijä', johon sähköntuotantopuolen on sopeuduttava olemalla valmis laskemaan energiantuotanto voimalaitoksilla. Ongelman korjaamiseksi meidän tulee uudelleen suunnitella sähköverkkoinfrastruktuuri siten että uusiutuvan energian tuotanto ei vaaranna sähköverkon vakautta ja hallittavuutta. Helpompi tapa hallita uusiutuvan energian tuotantoa on rakentaa älykkäitä mikroverkkoja, jotka ovat pieniä autonomisia sähköverkkoja, joilla on kaksisuuntaiset virransiirtomahdollisuudet. Tämä helpottaa sähköverkon operaattoreiden päätöksentekoa. Kaikkia pääverkkoon kytkettyjä mikroverkkoja voidaan ohjeistaa siten että niiden energiantuotanto ja energian kulutus edistää pääverkon vakautta ja varmistaa, että voimalaitosten sähköntuotantotarpeisiin ei synny liian nopeita muutoksia.</p> <p>Mikroverkkojen käyttöönoton lisäksi on kehitettävä työkaluja, joita mikroverkot voivat käyttää tasapainottamaan sähkön kysyntää, jotta sähköverkko kykenee selviytymään kaikista olosuhteista, joita voi seurata uusiutuvan energian tuotannon ajoittaisesta luonteesta. Esimerkiksi aurinkoenergian tuotantokapasiteetin lisääminen ei toimi korvaamaan perinteistä sähköntuotantoa tietyn pisteen jälkeen, jos voimme käyttää aurinkoenergialla tuotettua sähköä vain päivällä. Ratkaisu tässä on siirtää kulutus päivältä yöaikaan. Tätä varten meidän on kehitettävä energian varastointiratkaisuja.</p> <p>Tässä opinnäytetyössä tutkitaan mahdollisuutta hyödyntää jäähdytystä osana sähköverkon hallintaa käyttämällä kehittyneitä prosessin ohjausmenetelmiä yhdessä Internet-of-Things-lähestymistavan kanssa. Erityisesti tutkin ajatusta käyttäjä jäähdytysjärjestelmiä yksisuuntaisina energianieluina, joilla voidaan ajoittaa sähkökulutus uudelleen ajanjaksoihin, jolloin uusiutuvan energian tuotanto on huipussaan. Työn kohde on Oulussa sijaitsevan S-Market Tuiran höyry-puristusjäähdytyskierto, jonka kieroaineena toimii hiilidioksidi. Jarno Johannes Tenhomaa on johdattanut matemaattisen mallin vuoden 2016 diplomityössään dynaamisen lineaarisen aikainvariantin tilamallin, joka kuvastaa kierron dynamiikkaa siten kertoen jäähdytettyjen tuotteiden termisestä inertiaasta ja sitä kautta kierron sähköntarpeesta. Tässä työssä johdetaan malliennakoiva säädin (Model Predictive Controller) jäähdytysjärjestelmien dynaamista mallia hyödyntäen, jonka tehtävä on ohjata myymälän jääkaappien ja pakastimien ilman lämpötiloja, joita vuorostaan jäähdytettyjen tuotteiden lämpötilat seuraavat. MPC-säätö laskee jäähdytysjärjestelmän toimilaitteelle optimaalisen ohjauksen, jolla jäähdytysjärjestelmän lämpötila poikkeaa asetusarvosta mahdollisimman vähän valitun ennustushorisontin aikana.</p> <p>Lisäksi pyrin kehittämään ohjausstrategioita, jotka manipuloivat jäähdytysjärjestelmien virrankulutusta säätämällä vuorostaan malliennustavan säätimen asetusarvolämpötilaa. Näiden ohjausstrategioiden tavoite on varastoida joko halpaa ja / tai hiilineutraalia energiaa energianieluihin. Varastoitu energia voidaan myöhemmin hyödyntää aikoina, jolloin sähköverkon energia on kalliimpaa ja / tai tulee vähemmän hiilineutraaleista lähteistä. Energian Spot-markkinahintaan perustuva asetusarvon valintastrategia valitsee jääkaappien ja pakastimien asetusarvolämpötiloja Nord Pool AS:n Spot-hintatietojen mukaan. Sähköverkon uusiutuvan energian osuuteen pohjautuva asetusarvolämpötilan valintastrategia perustuu Energiategollisuus -etujärjestön julkaisemaan Suomen sähköverkon sähköntuotantotietoihin. Malliennustavan säätimen ja ohjausstrategioiden vertailuanalyysin tekemiseksi olen rakentanut reaaliaikaisen interaktiivisen simulaattorin Matlab-ohjelmaan, jolla pystyy havainnollistamaan supermarketin jäähdytysjärjestelmien toimintaa ja prosessin dynamiikkaa.</p>			

FOREWORD

I dedicate this work to my wife Lucinda and our daughter Joanna. Special thanks to my thesis supervisor István Selek.

Rauma, 7.12.2020. Janne-Pekka Nyman

TABLE OF CONTENTS

ABSTRACT.....	2
FOREWORD	4
TABLE OF CONTENTS.....	5
1 Introduction.....	7
2 The role of energy storage in demand response management	10
2.1 The role of energy storage in decarbonization of the power grid	12
2.2 Different control strategies for energy storage operation	13
2.3 Wind and solar curtailment and its restrictions on solar energy proliferation	15
2.3.1 Solar curtailment in California, United States	16
2.3.2 Solar curtailment in West Australia.....	18
2.4 The potential of energy storage for demand side energy management in Finland	19
3 CASE INTRODUCTION	23
3.1 Features of the vapor compression cycle	27
3.2 S-market Tuira complete model.....	29
4 MODEL PREDICTIVE CONTROL	32
4.1 The model predictive controller with QDMC algorithm	34
4.1.1 Quadratic programming.....	36
4.1.2 The MPC-control simulator algorithm	42
5 Description of MATLAB model.....	45
6 Temperature set-point selection strategies	51
6.1 Nord pool spot price -based temperature set-point selection.....	51
6.2 Power grid composition -based set-point temperature selection.....	53
7 RESULTS	59
7.1 MPC performance in refrigeration system.....	59
7.2 Control strategy benchmarks with simulations	60
7.2.1 Conventional Thermostat test results.....	61
7.2.2 Nordpool data test results	64
7.2.3 Energy source data test results.....	66
7.2.4 Nordpool data and energy source data test results.....	68
7.2.5 Results breakdown.....	70
8 Conclusions.....	72
8.1 Lessons for S-Market Tuira control strategy	72
8.2 Further development	73
9 REFERENCES.....	75

LIST OF ABBREVIATIONS AND NOTATIONS

CARIMA Controller Auto-Regressive Moving-Average

CAES compressed air energy storage

CHP combined heat and power -plant

DR demand response

HMI Human Machine Interface

LTI linear time-invariant

MPC model predictive controller

IoT internet-of-things

PID proportional–integral–derivative controller

QP Quadratic Program

1 INTRODUCTION

The decrease of the ecological footprint is crucial for the continuation of modern lifestyle as it is in the future. Therefore, the consideration of commonplace technological systems can make a big difference if we can find out how to make them even slightly more efficient. The electric grid is a vital infrastructure for countries, societies, and industries, and it has remained mostly unchanged in its core ideas for most of its over 100-years of history. In big systems, such as the electric grid, resource management and ecologically optimized implementation will generate large savings.

The renewable resources, such as solar and wind, are becoming increasingly important methods of carbon free energy production. However, they face limitations due to their inherent seasonal- and circadian rhythms, and thus the investment into carbon free renewable resources is only one part of the solution. The power grid has been using top-down architecture, where the aggregator side decides the amount of power generation done by the power plants since its introduction in the beginning of 20th century. In this model, the renewable energy is a disturbance, where power generation side must accommodate to the energy demand drop that the renewable power generation causes. As discussed by (DietmarBartz, 2018) p.32, power grid management is a challenging task to begin with, where further disturbances make the power grid manager's work of grid balancing increasingly harder. To fix the problem, we also must redesign the power grid infrastructure in a way that high portion of renewable energy does not endanger the power grid stability and controllability.

An easier way to manage renewables is by building smart micro-grids, which is an individual power grid with two-way power transfer capabilities, the benefits of which are further explained by (DietmarBartz, 2018) p.33. This results to easier decision-making on the grid aggregator side. All the micro-grids that are connected to the main power grid can be instructed how to accommodate their energy production and management to benefit the grid stability of main power grid, and to further improve the estimation of power generation demand of conventional power plants. Figure 1 illustrates the differences between conventional top-down grid hierarchy and two-way micro-grid hierarchy.

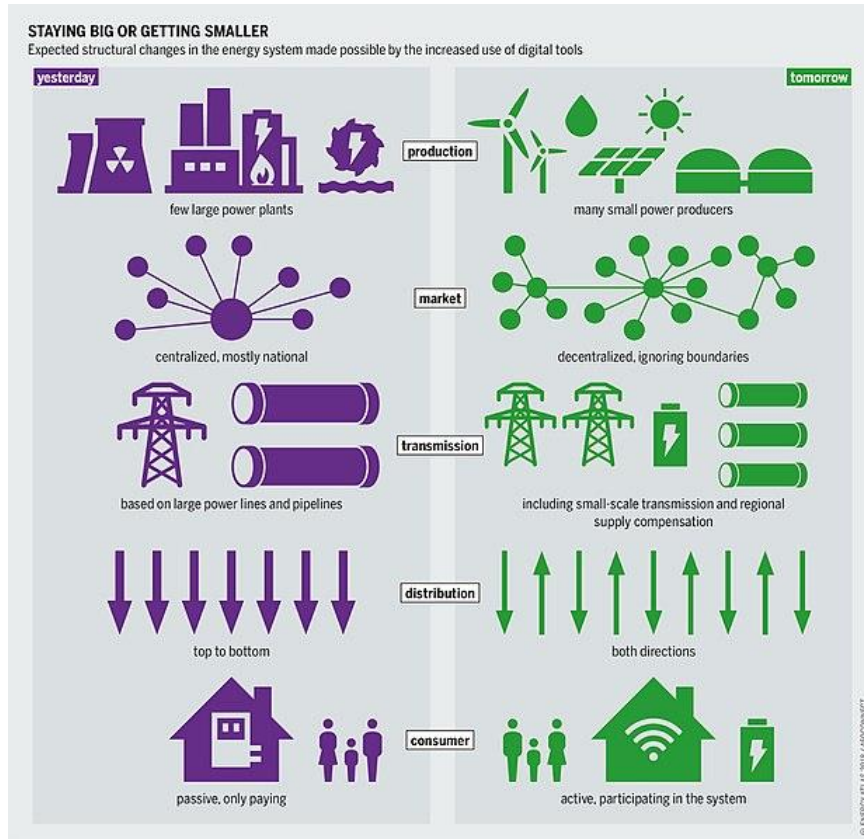


Figure 1. Differences between conventional power grid and smart grid. (DietmarBartz, 2018), p.33

Beyond the micro-grid introduction, the renewable energy proliferation faces limitations because of the intermittent nature of the renewable energy generation. Increasing the capacity of solar power generation will not work to replace conventional power generation after a point if we can only utilize the generated power during daytime. The solution here is to shift the consumption from daytime to night-time. To do this, we need to consider energy storage solutions.

In this thesis, I explore the possibilities of harnessing refrigeration to help power grid electricity management by using advanced control strategies combined with IoT approach. More specifically, I investigate the idea of using refrigeration systems as one-way energy sinks that can be used to time-shift the consumption of electricity by storing at peak renewable power generation periods. The target system is S-Market Tuira in Oulu, Finland, for which Jarno Johannes Tenhoma has built a mathematical model in his 2016 Master's thesis (Tenhoma, 2016). I formulated a Model Predictive Controller (MPC),

which uses Jarno's refrigeration system model, to control the temperatures of the stores coolers and freezers. Conventional thermostats strive to keep the controlled system in a set-point temperature. I strive to explore means of improving this by flexibly controlling power consumption of refrigeration systems, by in turn controlling the set-point temperature of a MPC controller. In this control strategy, the idea is to store either cheap and/or carbon neutral energy into the power sinks. The stored energy can later be 'recovered' from the energy sink at periods when the distributed energy in the power grid is more expensive and/or coming from less carbon neutral sources.

Additionally, I want to compare control strategies, that follow current electricity spot-prices and over-freezes the refrigerated goods when the price is low, and control strategies that incorporate considerations for power-grid renewable portion data and, in turn, over-freezes the refrigerated goods when the power grid energy is carbon neutral. The control strategies reacts to high spot prices and/or 'dirty' energy on power grid by raising the refrigeration temperature set-point up to a safe temperature where thawing will not begin, and food quality and safety is not compromised. The spot-price -based control changes the temperature set-point temperatures of the coolers and freezers according to Nord pool spot price data. Nord pool AS is power exchange market in Europe that offers both day-ahead and intraday power markets to its customers. The renewable portion data -based control strategies are based on power production data for the power grid in Finland provided by organization *Energiategollisuus*. Additionally, I have built a real-time interactive simulator in Matlab -program to illustrate the function and dynamics of the refrigeration systems of the supermarket.

2 THE ROLE OF ENERGY STORAGE IN DEMAND RESPONSE MANAGEMENT

The demand response (DR), or demand management, is based on the idea that the electricity user side should also partake in power grid stabilization. The DR is defined as by (Balijepalli, 2011) according to (Shafiei, 2015) p.2: “Changes in electric usage by end-use customers from their normal consumption patterns in response to changes in the price of electricity over time, or to incentive payments designed to induce lower electricity use at times of high wholesale market prices or when system reliability is jeopardized”.

Conventionally, power grid stabilisation has only been done by the grid aggregator side, who commands the power generation to ramp up or down according to power demand. However, the devices or micro-grid that participate in DR can ramp up or down their power consumption according to what best benefits the current state of the power grid. The goal here is to flatten the demand curve, so extreme up- or down-ramps are not required by the power plants.

The old model has worked for past 100 years so far, but along with the increasing popularity of renewable energy, which is often intermittent in nature, the power grid must adapt to handle more disturbances. As discussed in (Laura M. Arciniegas, 2018) p.1, grid-level energy storage, along with micro-grids, is an emerging technology that governments globally are considering to implement with the goal modernizing the power grid and decarbonizing it beyond the reach of the mere renewable energy production. Additionally, demand side management techniques such as load-shifting can be used to mitigate the limitations of wind and solar power generation caused by their intermittent nature, and therefore increase the renewable energy penetration level of the power grid.

In Figure 2, you can see an example of DR, where load-shifting is being used to flatten the electricity grid demand curve. Aside from grid stabilization benefits, the DR call event, where demand reduction is timed to happen, reduces emissions caused by running Peaker plants. Peaker plants are fast-ramping gas power plants or diesel generators that can respond to fast increased electricity demands, as in demand peaks. Peaker plants often use fossil fuels for power generation, and therefore reduction of their utilization

results in less emissions. In this scenario, the Peaker plant usage is replaced by ramping up conventional power generation later.

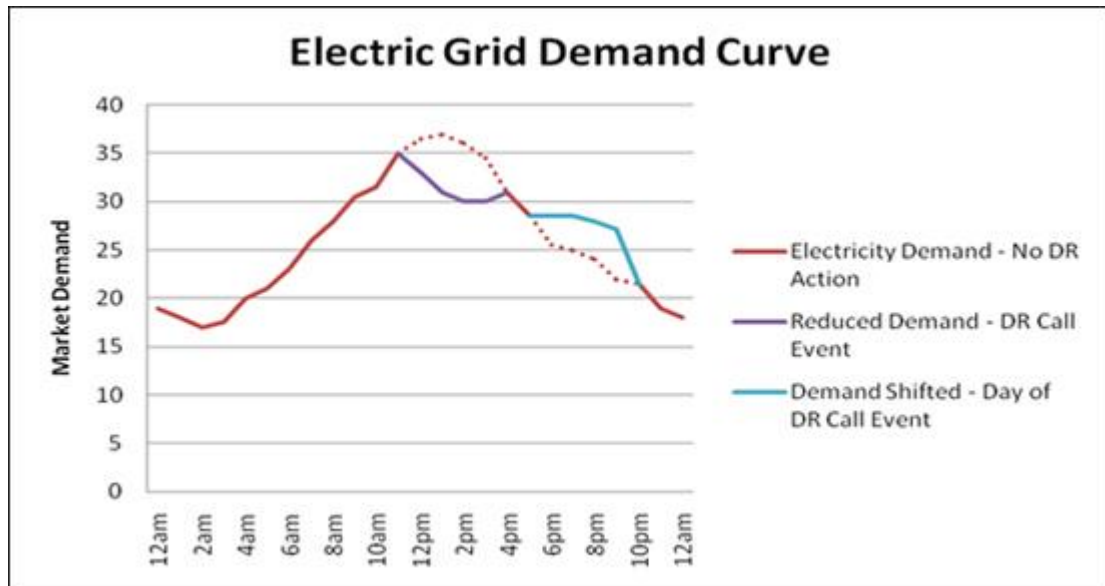


Figure 2. DR performed with the load-shifting technique. (LaMonica, 2014)

In (Laura M. Arciniegas, 2018) p.1 several energy storage technologies are listed, such as pumped hydro, compressed air energy storage (CAES), and batteries, used to store electrical energy. Therefore, devices that utilize these technologies can be upgraded to participate in DR. The devices include air-conditioners, industrial equipment, electric hot water heaters, electric vehicles, lights, dryers or, as investigated in this thesis, refrigerators.

The DR does not participate in energy efficiency considerations, where the goal is to lower the overall energy use of the devices. Instead, the goal of DR is to shift the energy consumption timing so that the power generation side can prevent causing additional emissions during peak power consumption hours. The important distinction here is that, while energy efficiency considerations are done on the level of an individual device, the DR considerations involve the efficiency of the whole power grid, and the carbon footprint of its electricity sources.

In this thesis I focus on energy storage potential of refrigeration systems as a DR method. In a broader perspective, the DR methods proposed in this thesis can be applied to other similar applications like building cooling systems with some degree of modifications.

2.1 The role of energy storage in decarbonization of the power grid

The energy storage is a highly potential technology for micro-grid power management in terms of outcomes for the carbon emission prevention. It can be thought of as the missing piece in the puzzle, on top of renewable energy and micro grids, which could allow the society to be powered completely by renewables in the future. However, much more important than the proliferation of energy storage is its correct utilization. As discussed in (Laura M. Arciniegas, 2018) p.2, even though the bulk energy storage is generally considered an important contributor for the transition toward a more flexible and sustainable electricity system, it is not fundamentally a “green” technology by itself, and it doesn’t lead to reductions in greenhouse gas emissions unless it’s specifically operated towards that goal.

Bulk energy storage often provides several services at once for the energy system. In (Laura M. Arciniegas, 2018) p.1, the further benefits of energy storage are explained. In addition to increased renewable energy penetration on the power grid, other benefits include the reduced need for Peaker plants, optimization of congested transmission, improved frequency regulation service, electricity demand management and a distributed energy storage can provide power while system operations are restored in the case of a natural disaster. Collectively, the result is that power grid aggregators can more easily deal with instabilities, because shifting consumption away from peak times flattens the power demand curve over the circadian period and this reduces the amount of up and down ramping the conventional power plants have to do.

Household electricity storage has boomed recently along with popularity of Tesla Powerwall and electric vehicle batteries, which are used as an energy storage for smart micro-grid solutions. The electric car batteries can likewise work towards this purpose. In the case of batteries, power can travel to both directions and can be recovered to provide peak electricity for power grid. However, the energy storage processes in buildings and households can go beyond mere batteries. Other techniques include smart

control of building heating, water heaters and, as I consider in this thesis, refrigeration. These devices have the further functionality beyond mere energy storage purpose, and they are essential to have in households and businesses, so improving their functionality is a big deal. The idea here is that even though one item wouldn't make a huge difference in grid stability by itself, if we were to upgrade all power consuming items over time with internet connection, we will be able to convert all devices into part of the power grid. In this approach, the group control of power consuming devices allows each individual device to take part in ensuring the grid stability. Ideally, this will allow the power grid to mitigate the intermittent nature of renewable power generation. Hence, it will allow us to cut down on carbon-based fuel consumption, which is currently by far the biggest threat to environment as of now.

2.2 Different control strategies for energy storage operation

The key variable for environmental impact outcome for batteries and other storage methods is timing in relation to carbon neutrality of the electricity available. The problem has always been coordination between available electricity sourcing data and decision making of the electricity storage devices. However, with the popularization of Internet-Of-Things (IoT) approach as more and more of appliances, homes, buildings, and industrial facilities are wired to the internet, it is easier than ever to synchronize the consumption of devices to follow optimized consumption patterns. Here the goal of the consumption time-shift optimization is to minimize the carbon emissions of the power production. The outcome of carbon emission minimization depends on available data and how well the data represents the momentary portion of electricity on the power grid that has been produced with carbon free methods.

A straightforward way to implement DR is to follow the electricity spot price in energy markets, where the spot price reflects the carbon footprint of the current state of the electricity on the power grid. However, to successfully acquire carbon emission reductions through the implementation of this strategy requires political will in the energy market to penalize carbon emissions over clean energy. As discussed in (Kim, 2010) p.1, this has been implemented through carbon taxes, which works to raise the electricity prices in spot price markets, such as *Nordpool*, when the electricity on the power grid is

produced through carbon intensive methods. Nord Pool AS is a European power exchange market that offers day-ahead and intraday energy trading.

When the spot price reflects the carbon footprint, an emission suppression can be achieved by consumers, who shift their energy usage according to the time-based rates. This has become an increasingly popular method of saving money for consumers. Individual consumers who possess numerous solar panels can even earn money if their power output or energy storage capacity is high enough to surpass their own consumption. For example, in (Schneider, 2009) p.2 Schneider electric claims that participants of their DR program can earn back up to 5-25% of their annual electric energy costs.

So, the conventional strategy for energy storage operation has been based on the idea that in power grids with large portion of renewable energy production, a burst of wind or daytime solar power production can be experienced as drops in electricity spot price. However, other data sources than just mere energy spot price data is necessary to confirm the conditions for renewable generation. The researchers have pinpointed instances, where assimilation of energy storage has had the counterproductive outcome of increased grid emissions. In (Eric S. Hittinger, 2015), according to (Laura M. Arciniegas, 2018), p. 2 it was found that bulk energy storage would consistently increase electricity system emissions when operated to maximize revenue. One of the reasons leading to this is, that as any electricity system does, also energy storage exhibit losses due to inefficiency. Discharging a battery will always output less than 100 % of the electricity that was used to fully charge it. Therefore, utilization of batteries will always increase the total amount of electricity passing the electricity system. In the study (Lueken, 2014), that focused on a power grid on the east coast of United States called PJM interconnect, it was concluded that integrating 20 GW of storage had multitude of positive effects for the residents including lowering the electricity costs annually by 2,5 billion dollars. However, a life cycle emission analysis found a modest increase in greenhouse gas emissions. As stated by (Laura M. Arciniegas, 2018) p.2, when the storage device has 75% round-trip efficiency, the off-peak power needs to be at least 33% cleaner than peak generation to prevent adding further emissions to the grid.

According to (Laura M. Arciniegas, 2018) p.1, CO₂ emission related to battery storage of electricity could be decreased significantly (25-50%) with little cost penalty (1-5%), when

the energy storages are operated with strategies that value both revenue and CO₂ emission minimization. A control strategy that is focused on carbon emission minimization can result in major decrease in environmental impact in comparison to a control strategy following only the electricity spot price, even though the customer may pay marginally higher energy costs. Only a small shift legislation (for example cutting of fossil fuel subsidies, which totalled International Monetary Fund (IMF) report estimated to have been 6.5 percent of global GDP (\$5.2 trillion) in 2017 (Clayton Coleman, 2019), p.2) could likewise tip the economic considerations to favour carbon emission minimizing control strategies.

2.3 Wind and solar curtailment and its restrictions on solar energy proliferation

Wind or solar curtailment is a problem that the energy storage could help to fix very effectively. In areas, where wind or solar curtailment frequently occurs, investments into properly operated energy storage should be made before further power generation capacity investment can pay off. In (Lew, 2013), p.4 curtailment is defined to broadly refer to momentarily utilizing less wind or solar power generation capacity than is potentially the maximum electricity production output of existing wind or solar power generators. In practice, solar curtailment means, that solar panels must be turned off to prevent overloading the power grid. In (Aho, 2012) according to (Denholm, 2015), p.1, it is explained that wind curtailment is an action that is performed by reducing the energy captured from the wind by changing the blade pitch angle of the wind turbine. Wind and solar integration studies have predicted increased curtailment as the renewable power generation penetration level increases on the power grid. The numerous reasons leading to curtailment are, for example, transmission congestion, or local network constraints, can prevent transport of energy to load stations, especially from new renewable power generation sites. The power grid infrastructure may not be adapted to back-feeding of electricity without voltage control issues. Non-synchronous generation may be limited for the grid. The most relevant dynamics for this paper are the minimum operating levels for thermal- and hydro power plants, which is the problem that will be discussed in the context of curtailment.

2.3.1 Solar curtailment in California, United States

An example of solar curtailment from (CAISO, 2016) p.2, is illustrated in figure 3, which depict power demand curve from grid manager's perspective in a high solar power generation region such as California, United States. This shape is nicknamed the "Duck curve" and it is caused by day-time peak in solar production, which reduces the day-time electricity demand.

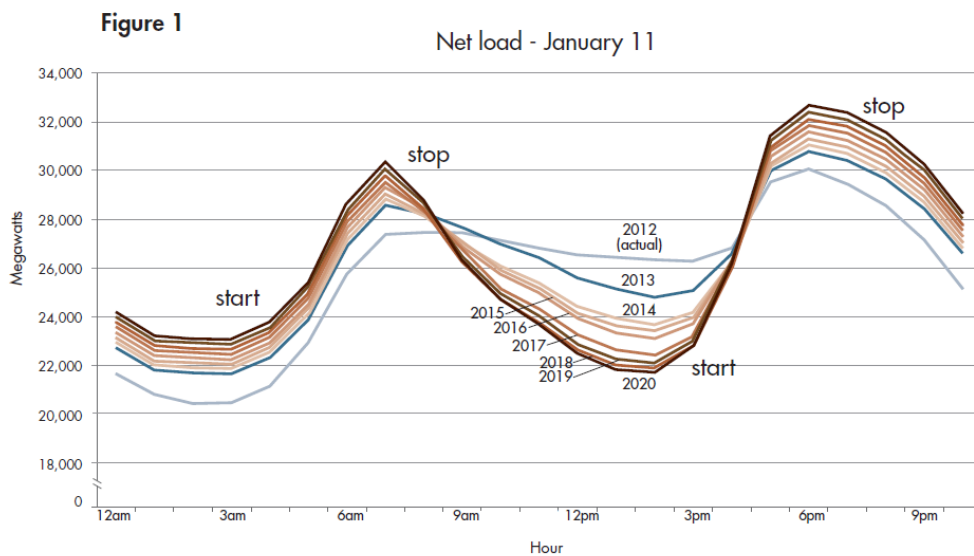


Figure 3. The "Duck curve", where solar production causes a notch in grid electricity demand during day-time peak production. (CAISO, 2016), p.2.

For comparison, Figure 4 includes all energy consumption in the power grid and depicts the portions of electricity produced by solar power and conventional power plants. In Figure 3, the power demand peak around 7 am in the morning, when people have woken up and start consuming power, but the sun is still down, and solar power production has not started. During daytime power generation demand plummets due to solar generation, but when sun goes down, the power demand peaks again. Wind curtailment can work similarly to solar curtailment, but wind generation patterns tend to be even less periodical in their behaviour, even though in some regions wind tends to be stronger during night-time.

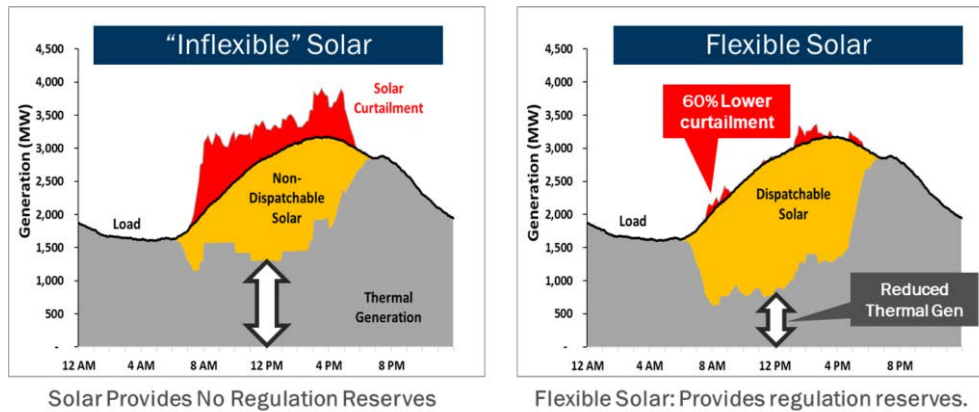


Figure 4. Overproduction of solar power drives solar panels to be shut down in a non-flexible power system. This is called solar curtailment. (Mahesh Morjaria, 2019)

The conventional baseload power plants must be run continuously to make sure they stay at their optimal efficiency. They do take part in grid stability planning, but rather than using them for DR, the planning is done around them. As discussed in (Denholm, 2015) p.4, the baseload power generation rate means the minimum power output the power plants participating in a grid operation can produce when ramped down to lowest operation capacity without shutting down. The conventional power plants are rarely completely shut down, because starting up and up-ramping can take hours. If they were to be shut down in response to peak solar generation during day-time, they would not be able to start up in time to keep up with the sharp increase in power demand, which comes in the evening when sun goes down and solar generation ends.

Problems can arise during daytime, when demand for conventional power generation plummets to the level of the baseload generation. In this situation, the only way to prevent causing damage to the power grid is to shut down solar panels until power demand is equal to base load power production. This complicates the grid management job and leads to a bottle neck phenomenon, where increasing the amount of solar or wind power generation capacity will not increase energy production after certain point. Instead of shutting down the solar panels, the energy storage devices can increase the energy consumption and capture the excess of solar energy, the consumption of which can in turn be shifted to night-time. This is called the load-shifting strategy, where we utilize energy storage to shift the timing of solar power consumption from daytime to night-time.

Another problem occurs at evening when sun goes down and solar production stop. The peak in power demand occurring at evening will become especially challenging with increased reliability on solar power. Power demand can peak fast because people are still consuming plenty of electricity after dark. The response to peaking power demand is often handled by flexible power generation units, such as 4-stroke diesel engines or natural gas Peaker plants. This is because diesel engines and gas burners are extremely fast at starting and ramping up compared to conventional power generators in power plants.

At the evening, discharging the stored energy would be reflected as flattening of the evening peak in the figure 2 demand curve. All the power consumption that is prevented by the discharge of energy cutting demand will in turn reflect in lowered peak electricity demand. Therefore, energy storage will work to reduce carbon-based fuel consumption by saving excess solar power generated during the day and shifting the consumption to a peak-demand period at the evening.

2.3.2 Solar curtailment in West Australia

Another well-known case of solar curtailment can be found in West Australia, where implementation of demand side energy management could be utilized urgently to help prevent a big grid stability problem in very near future. As discussed in (Mercer, 2019), the West Australia is one of the sunniest landscapes in the world and there the rooftop solar power generation has been an incredible success. Due to very long distances, the state of West Australia's power grid is virtually a power island, with little power exchange to other grids.

The heart of the problem in West Australia is that the solar panels are not smart solar panels. Instead they are mostly 'dumb' solar panels, which cannot be turned off by the grid aggregator and constantly produce power. In the event, where power generators have been ramped down to baseload production, and solar generation still exceeds power demand, grid managers have to make the undesirable decision of shutting down entire power plants in order to protect the grid from overloading. If the baseload floor of 700 MW is breached, the result can be rolling blackouts. The power generators must be shut down and grid stability controllability is lost, until solar generation goes back down again. In the event, where solar generation goes down, new problem emerges with the high

ramp-up times of the power generators. These problems can result in system-wide blackouts.

Here the urgently needed solution is smart solar generation, where panels are equipped to follow aggregator demand. Enough solar panels need to be able shut down in the case, where solar generation would breach base-load power generation. However, a complementary approach is the implementation of demand side energy management. This approach helps not only with the core problem of grid stability, but it also helps the power grid to increase the portion of renewable energy utilization at the power grid overall. At the point, where solar generation breaches the baseload floor, increased energy consumption can help to prevent power plant shutdowns. The benefits are two-fold, the power plant shutdowns can be avoided, and solar panel shut down can be avoided also, when solar power consumption is shifted from daytime to night-time. Here we not only help to stabilise the power grid, but also reduce overall carbon emissions by increasing the solar power penetration of the power grid. Additionally, we will overcome the bottleneck phenomenon, where further investments into power generation does not anymore yield as much renewable power to the power grid. A solution could be a combination of IoT –approach and advanced control algorithms, which are capable of correctly timing the storing and discharging of energy storages.

2.4 The potential of energy storage for demand side energy management in Finland

As the case study subject, S-Market Tuira, is in Finland, knowing the power grid composition here is important for understanding how to implement energy storage correctly towards the goal of emission reduction. The Figure 5 illustrates an example of distribution of power generation in Finland by different sources. Data is from the organization *Energiateollisuus*, which records power generation and consumption in Finland. In this figure, we can see the continuous nature of power generation by, especially, nuclear power and Combined Heat and Power (CHP) -plants, along with other conventional power generation. Wind power produces by itself a significant portion of consumption during windy periods. However, the intermittent nature of wind power generation is on display here. DR is met by hydropower, energy import and CHP -plants. Here the hydro power and electricity import can be observed to be used to balance the

difference between day- and night-time electricity consumption. CHP -plants are used to respond to demands of base load electricity demand variation. Wind power generation can be observed as a slight decrease of CHP energy generation.

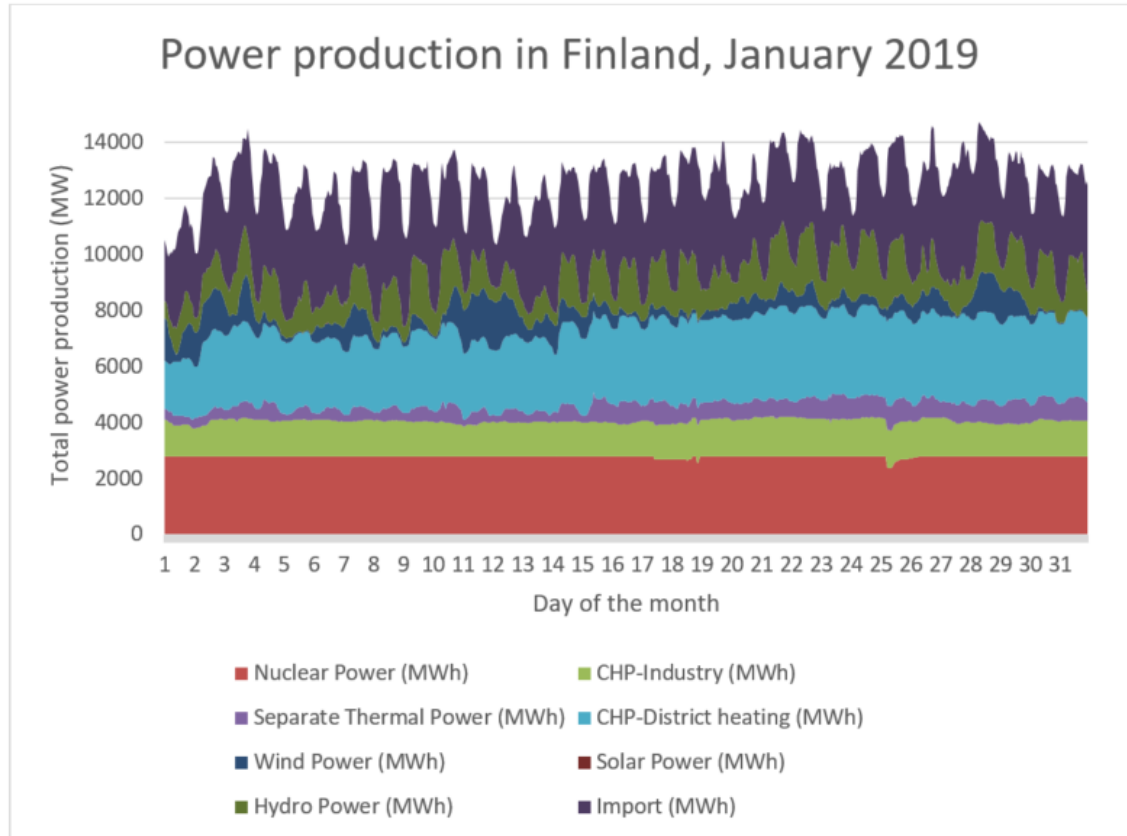


Figure 5. Power production in Finland in January of 2019. [Based on data from *Energiategollisuus* (Energiategollisuus, 2020)]

As seen in Figure 5, in Finland we do not have solar power on the same scale as California or West Australia, but we have significant amount of wind power generation. Wind power generation is intermittent in nature, and therefore other power generation always must react by down-ramping when a burst of wind occurs. Advanced freezer control can allow for higher wind energy capture through higher power consumption through increased freezing at the moment of peak wind power generation. Widespread advanced control in combination with IoT could in future allow higher overall wind power generation at times when some windmills would otherwise need to be turned off to prevent power grid overloading. The consumer side electricity management will reduce the need of

utilization of flexible fuel generation, which is often more expensive than base load power generation.

A more visible aspect of large-scale utilization of freezers as part of grid management would be expected to be a dampening of power consumption peaks. This would appear as lessening of the difference between day and night electricity consumption levels. This will make power grid stabilization easier for grid managers, and in turn, tolerate more disturbances to the power grid, which the intermittent nature of renewable power would produce.

The power grid composition in Finland has variety in terms of power generation methods, as illustrated in Figure 5. The grid has good controllability potential for stabilization, as combined heat and power plants can be ramped up and down, hydroelectric power dams have good load shifting capabilities and the power grid is connected to neighbouring countries, from where Finland currently purchases considerable portion of its power. However, it has been long term strategy for Finland to reduce reliability on foreign energy, which is expected to be accomplished by nuclear power. The nuclear power plant Olkiluoto 3 is expected to be finished by 2021, which is world's first European Pressurised Reactor (EPR) project in the world. Olkiluoto 3 will have power output of 1600 MW, which will increase the total nuclear power production by almost 60 %. Beyond this, Hanhikivi 1 nuclear power plant is planned to be in the municipality of Pyhäjoki, which will have capacity of 1200 MW. Possible additional projects include Olkiluoto 4 and Hanhikivi 2. Therefore, Finland will be heavily invested in nuclear power generation in the future, which is undoubtedly good in terms of carbon emission prevention. According to (Pehl, 2017) p.941, each kilowatt hour of electricity generated over the lifetime of a nuclear plant has an emissions footprint of 4 grams of CO₂ equivalent (gCO₂eq/kWh), which ranks it on equal footing solar and wind power.

The effect this will have for the power grid is, that base load power generation will increase considerably. First, this will allow Finland to cut down on electric power imports. Secondly, combined heat and power plants can be run at lower loads. This will result in carbon emission reduction, as combustion of fuels is replaced by carbon free energy. However, the nuclear power plants are not conventionally used for up- or down ramping electricity production and therefore the increase of base load power generation may result

in a situation, where power grid managers may have less flexibility for responding to disturbances in power grid. In this situation, smart micro-grids with storage capacity can help to flatten the demand peaks and drops by time-shifting power consumption. Along with increased nuclear power generation, the base-load power will have lower carbon footprint. Therefore, the key-requirement for storage utilization, that off-peak electricity is at least 33% cleaner than peak generation, a requirement proposed in (Laura M. Arciniegas, 2018), p. 2), will be easier to attain. Especially in cold winter months, storing the cleaner day-time electricity can help to shave off night-time peak electricity consumption, which is caused when the night-time temperatures will drop under $-30\text{ }^{\circ}\text{C}$ and building heating has to work much harder.

To maintain good power grid stability in Finland, DR can be implemented to the power grid by controlling smart storage devices with advanced load-shifting algorithms. Flexible energy storage control can be a money saving technique for a customer because it can help to shift energy consumption to low electricity price times. If Finland will start exporting the excess power, the power generation strategy may stay similar as it is currently. But if Finland consumes the additional power domestically, down ramping of conventional power plants is inevitable because the grid always must consume all of the base load power generation. Especially when more renewables are introduced to this balance equation, energy storage can become a necessary tool for grid balancing.

3 CASE INTRODUCTION

The case study for this thesis work is the supermarket S-market Tuira, located in Oulu, Finland. The subject has been studied in Jarno Johannes Tenhoma's MSc thesis (Tenhoma, 2016), Development of a Dynamic Mathematical Model for Demand Side Management of the Grocery Store S-Market Tuira. In this chapter, I summarise the relevant parts of Jarno's thesis, as my thesis considers the same system and I will use his model of the refrigeration dynamics of the basis of my MPC controller formulation in the next chapter. The store in subject is a "middle sized" supermarket with a service area of 2500 m². The construction of the store was finished in December 2015 replacing the old S-Market, which was built at the exact same location.

The supermarket was built with implementation of environmentally friendly technologies in mind. Additional benefit of this is the research possibilities offered by the solution in addition to the achieved environmental benefits through clean technology. The figure 6 illustrates the store micro-grid architecture, which can be monitored in real-time at the Tuira S-Market smart grid website (VTT, 2020). The website was built in cooperation with VTT (Technical Research Centre of Finland Ltd). S-Market Tuira has its own micro-grid, solar power generation with photovoltaic solar panels and a vapour compression cycle, which uses CO₂ as the working fluid.

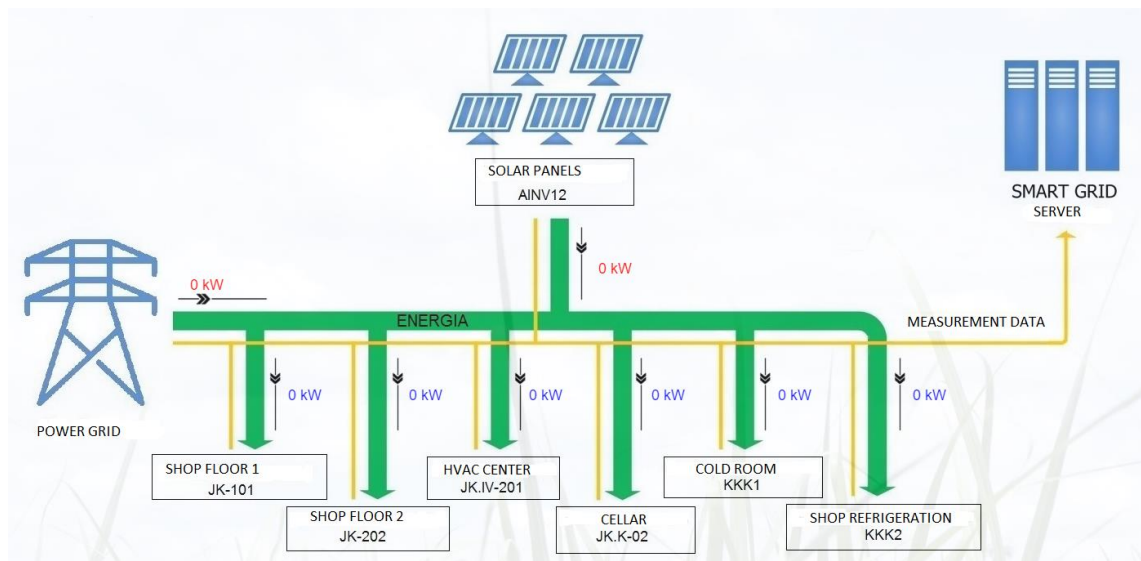


Figure 6. S-Market Tuira energy balance in the micro-grid architecture. (VTT, 2020)

In (Tenhomaa, 2016) p.11 it is explained, that the supermarket has a centralized vapour compression cycle that performs variety of tasks within the market, such as refrigeration and building heating, hot tap water heating and geothermal power recovery through heat wells. In addition, there are heat pumps and heat collecting solar panels in the system to maximize energy efficiency and environment friendliness.

Important feature in terms of environmental impact is that the vapour compression cycle uses CO₂ as refrigerant instead of the contemporaneously more common R-22 (Chlorodifluoromethane). Using CO₂, or R-744, as work fluid for refrigeration systems is by no means a recent idea of the modern engineering era, but it has not had widespread commercial use since the 1930s. Adopting CO₂ as working fluid for vapour compression cycle is significant, because it is nontoxic, doesn't have impact on ozone layer depletion and, most importantly, doesn't have high global warming hastening potential compared to conventional refrigerants, like fluorocarbon chemicals (R-12 and R-22), in the event that it should leak to the environment. Heat capacity of CO₂ allows for good refrigeration capabilities; however, the equipment must be built to handle higher pressures. For example, the high-side pressure of R-22 cycle is around 17 bar, whereas CO₂ cycle uses pressures up to 65 bar in the case of S-Market Tuira. Therefore, retrofitting R-22 vapour compression cycles to work with CO₂ would not be possible.

In recent years, CO₂ has become an increasingly important refrigerant in the food industry. As explained in (Danfoss, 2009) p.3, it is one of the few sustainable refrigerants for supermarket systems from an environmental and safety perspective. It is very abundant in the environment and it is considered a waste product from variety of production processes, and therefore its cost is extremely low, and it is easily available anywhere. However, it is heavier than air and therefore, it can accumulate in the lower parts of a non-ventilated ambient, especially in basements, causing suffocation due to lack of oxygen. CO₂ is an inert gas, so it is compatible with all common materials encountered in a refrigerating circuit, be it metals and plastics or elastomers.

The store uses heat pump technology extensively in its centralized vapour compression cycle. Benefits of a centralized CO₂ vapour compression cycle is that the same system includes both building heating and refrigeration. The working fluid cools down when it expands in volume. The temperature difference between the working fluid and the air

inside the refrigerator causes the heat energy to be removed from the refrigerator. The heat well works similarly; the expanded working fluid becomes colder than the temperature underground, and therefore it leaches energy from the ground. The gathered energy is directed to the shop interior or at the tap water heating boiler. Once the working fluid has released the absorbed heat energy, it can be expanded again to low pressure so that it is ready to absorb more energy. The heat well acts as heat source, which is used to maintain the heat balance of the building. This solution allows the building to self-sustain its heating without being connected to district heating system or having additional electric heaters.

Advanced refrigeration systems, like the CO₂ vapour compression cycle, have become increasingly widespread. Here lies an opportunity to perform load control with the supermarket refrigeration systems power consumptions by utilizing DR control strategies. According to (Tenhoma, 2016) p.12, (Rivers, 2005) and (Hovgaard T. G., 2011) found out that the main fraction (50-80%) of a supermarkets total energy consumption is due to refrigeration and heating systems. Therefore, further consideration into refrigeration efficiency and control strategies is warranted, because wide implementation of improved refrigeration control has big potential. For example, in Denmark, which has around 5.5 million inhabitants, there are about 4,500 supermarkets consuming approximately 550 GWh annually (Hovgaard T. G., 2012a) p.1. This means each store consumes on average around 62.8 MWh per year. Collectively, the supermarket refrigeration accounts for around 2 % of the nation's total electric power consumption alone. Therefore, it can be concluded, that refrigeration system shares a great potential for demand reduction and development of consumption flexibility, by using advanced control strategies, needs to be explored further.

S-market Tuira is an existing real-life DR application of a supermarket refrigeration system. Flexible power consumption -control strategy, in the case of S-Market Tuira, is realized through the store's vapour compression cycle, which is enables refrigeration and can additionally be used for building heating. The vapour compression cycle amounts to a major fraction of the total energy consumption of the supermarket. Due to large amount of perishable food items that must be stored and refrigerated, the supermarket has a significant "one way" energy storage potential. Combination of the storage potential, vapour compression cycle offers great opportunities for control flexibility. Figure 7 is a

simplified process flow -chart of the different vapour compression cycle stages of the S-Market Tuira.

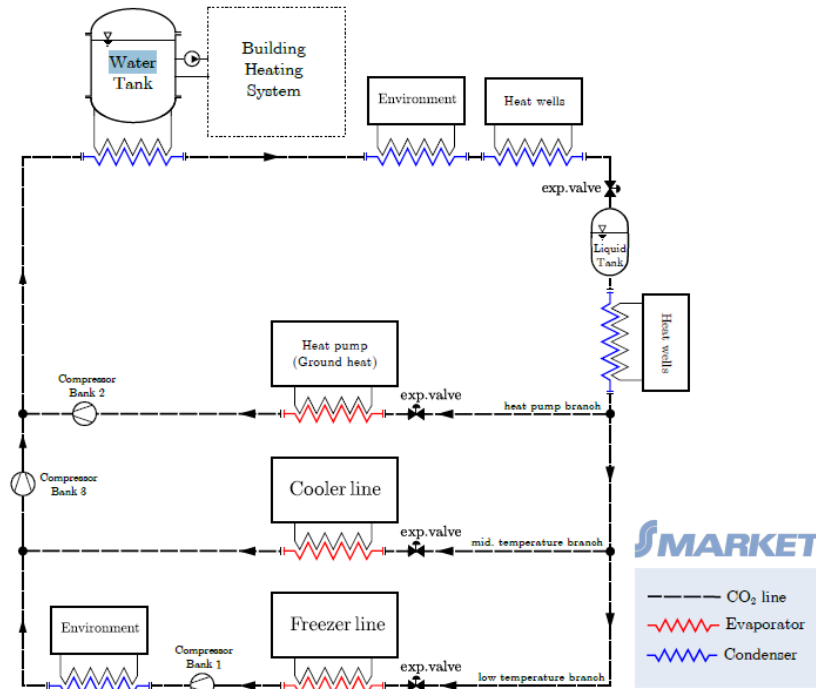


Figure 7. Feature of the vapour compression cycle used in S-Market Tuira. [J. Tenhoma]

As discussed in (Tenhoma, 2016) p.20, understanding the refrigeration dynamics and related phenomena is essential to realize how to exploit the refrigeration system for the benefit of demand side management. The dynamic behaviour of the process is captured by developing a mathematical model which adequately describes the relevant physical phenomena. Building a process simulator based on obtained mathematical model can help to visualise process behaviour on relevant scenarios, but the most important benefit for model-based approach is that operation of the system can be controlled optimally by iterative algorithms, such as MPC.

The dynamic modelling for energy balance of the vapour compression cycle and interacting subsystems is done in (Tenhoma, 2016). In my work I have used the resulting thermodynamic system models as a basis for building an interactive simulator, which can

be controlled by MPC and can be experimented with to benchmark different refrigeration control strategies.

3.1 Features of the vapor compression cycle

Figure 8 is a screenshot from Human Machine Interface (HMI) system of S-Market Tuira, which was presented in (Tenhomaa, 2016) p.18. This is described in (Tenhomaa, 2016) in more detail, but I will describe the main process conditions here.

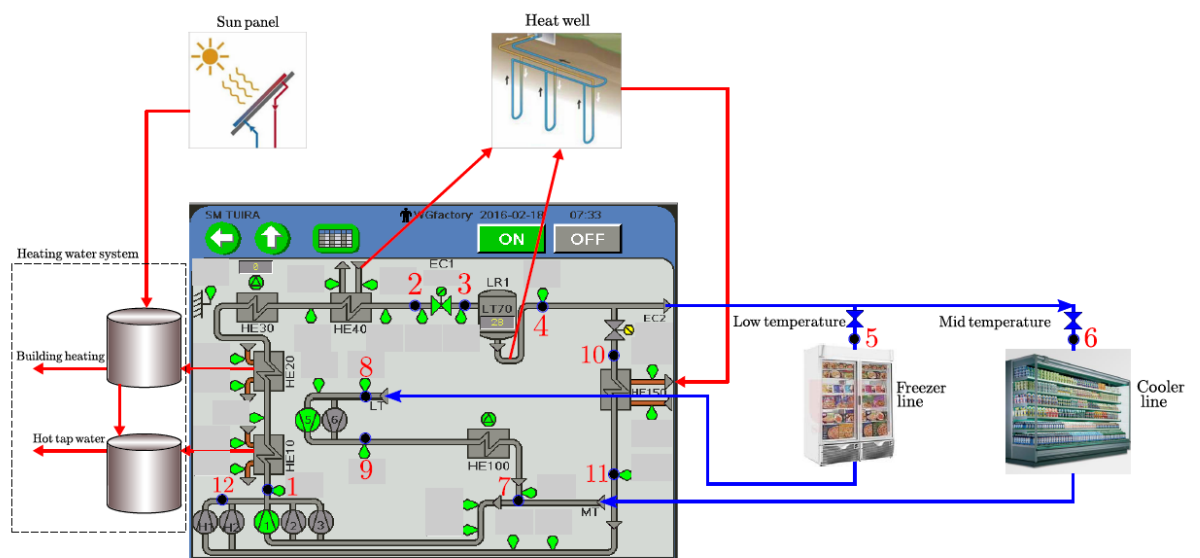


Figure 8. Vapour compression cycle of S-Market Tuira. (Tenhomaa, 2016) p.18.

Stages of the vapour compression cycle are:

1. Compressor unit discharge side
2. End of condenser line.
3. Discharge side of liquid tank's discharge valve
4. Discharge side of the liquid tank.
5. Cooler cabinets and cooler rooms expansion valves.
6. Freezer rooms and freezer cabinets expansion valves.
7. Stage 5 to 7 represents the heat transfer from cooled goods to the low temperature CO₂.

Figure 9. Vapor compression cycle pressure - enthalpy diagram. Blue and green paths represent mid, low temperature branches and heat pump branch respectively. (Tenhomaa, 2016) p.19.

3.2 S-market Tuira complete model

The purpose of mathematical model for the S-Market Tuira is to reveal the heating and cooling dynamics of the supermarket refrigeration systems. In upcoming chapters, I utilize these modelled dynamics as a basis for a model-based optimization algorithm.

As discussed by (Tenhomaa, 2016) p.23 law of physics states that mass can store heat energy determined by the item's heat capacity. Therefore, mass of the items can be also identified as heat buffers. The size and properties of these buffers determine the major fraction of the heating and cooling dynamics of the market. These buffers may be various things such as food items and building materials. The dynamical model is needed to provide accurate predictions about the market's refrigerator systems electricity consumption. The prediction is used to make decisions about whether to increase or decrease the energy consumptions to optimize cost efficiencies during the upcoming future time window.

The modelling principles and related equations of each refrigerator system are detailed in (Tenhomaa, 2016). S-Market Tuira has 20 refrigerator system, 4 of which are freezers and 16 are coolers. The methods of deriving the system model are detailed completely in (Tenhomaa, 2016). The principal idea for the model parameter identification for freezers is, that observing the effect of a scheduled event called defrost for the freezer temperature trend. Defrost event appears once in approximately 8 hours for all refrigerator units. The purpose of defrost is to remove the ice deposit from the evaporator coils. The length of the defrost event is approximately 40 minutes on average (varies unit by unit), during which temperature is monitored. The obtained temperature trends were used to build linear time-invariant (LTI) -models for the observed systems.

I used these models in my work to simulate the refrigeration system and formulation of MPC. Temperatures of air and goods contribute to the state of thermodynamic model in each refrigerator. The mathematical model of the vapour compression cycle of S-Market Tuira has the following state-space form:

$$\begin{bmatrix} \dot{T}_{air}(t) \\ \dot{T}_g(t) \end{bmatrix} = \begin{bmatrix} -(\hat{\alpha}_{ga} + \hat{\alpha}_{ea}) & \hat{\alpha}_{ga} \\ \hat{\alpha}_{ea} & -\hat{\alpha}_{ga} \end{bmatrix} \begin{bmatrix} T_{air}(t) \\ T_g(t) \end{bmatrix} + \begin{bmatrix} \hat{\alpha}_{ea} \\ 0 \end{bmatrix} T_{env}(t) + \begin{bmatrix} \beta \\ 0 \end{bmatrix} \sum_{i=1}^N f_u(u_i(t)) \quad (1)$$

where the vector $[\dot{T}_{air}(t), \dot{T}_g(t)]^T$ (the average temperature of the air column and the average temperature of refrigerated goods) represents the state of the refrigerator. Applying state augmentation, the thermodynamic model has the form:

$$\dot{x}(t) = Ax(t) + B\tilde{u}(t) + DT_{env}(t), \quad (2)$$

where $x(t) \in \mathcal{R}^{40}$, $\tilde{u}(t) := [f_{u,1}(u_1(t)), \dots, f_{u,41}(u_{41}(t))]^T \in \mathcal{R}^{41}$ for all $i = 1, \dots, 41$ corresponds system's state including temperatures of air and goods. The $u_i(t) \in [0,1]$ term corresponds to system's scaled inputs relating to the opening degree of expansion valves. The term $w(t) \in \mathcal{R}$, in turn, corresponds average temperature of the shop inside air at time step t . The discretising the formula (2) gives:

$$x_{k+1}(t) = Ad * x(t) + Bd * \tilde{u}(t) + Dd * T_{env}(t), \quad (3)$$

Thus, the relationship between system model and system control output is of the form:

$$y_{k+1} = Cx_{k+1}.$$

This system in (3) is subjected to the following constraints:

$$x^{min} \leq x(t) \leq x^{max}, \quad (4)$$

$$0 \leq \tilde{u}(t) \leq 1, \quad (5)$$

for all $t \in \mathcal{R}$. The vectors x^{min} and x^{max} represent temperature boundaries for all refrigerator units. The first constraint (4) restricts the temperature of the air column and consequently the temperature of the refrigerated goods in each refrigerator to be within acceptable temperature boundaries. For a freezer, for example, the temperature is restricted between -33 °C and -15 °C. The second constraint (5) represents the expansion valve opening degree restrictions. The electric power consumption of the vapour compression cycle (i.e. hydrodynamic model) has the following form:

$$P(t) = h_0 v(t) + h^T \tilde{u}(t), \quad (6)$$

where $v(t) \in [0,1]$ denotes the opening degree of the expansion valve located at the heat pump branch, h_0 and h are constants of appropriate dimension ($()^T$ denotes the transposition operator). Variables $v(t)$ and $w(t)$ are treated as exogenous i.e. these originate externally and unexplained by the model. (It is assumed that the future trajectories $v(t)$ and $w(t)$ are known or can be forecasted with sufficient accuracy).

4 MODEL PREDICTIVE CONTROL

The MPC, also known as receding-horizon control, is an advanced method of process control that was first implemented in practice in the 1980s for process industries, such as chemical plants and oil refineries. More recently it has been utilized as a control strategy for further development of power system balancing models that are capable of inclusion of renewable power generation that is intermittent in its behaviour. The MPC is virtually always implemented as digitally, although specially designed analogue circuitry has been researched. In the first couple of decades the implementation of MPC was hindered by computer processing power limitations. However, along with the higher computer clock speeds of common computers from 21st century, machines capable of running real-time MPC computation have become readily available to everyone.

MPC is not a specific control algorithm, but rather a systematic approach to problem solving. As discussed in (Rossiter, 2003) p.1, The goal of many effective control strategies is to mimic the approach of human behaviour, because humans are fairly good at control. This is due to multitude of inherent abilities and learning capabilities that we as people take as granted in everyday life, but that are often very complicated to implement into a computer algorithm. For example, conventional PID-control can be deconstructed as a simplification of a human technique for controlling simple systems without the ability predict the system behaviour, but rather by reacting to changes. Humans anticipate, in other words predict, the future behaviour of controlled system with a mix of sensory input, such as eyesight, and learned knowledge about controlled system. Again, this is intuitive to us and we do not have to make effort to do it, but rather it is a result of practice. In practice, prediction can be something so simple as to approaching a tight curve while driving a car. Through eyesight, we see the curve coming up and therefore know that we must apply brake before arriving to the curve, so the car keeps traction. In this situation a PID-controller tasked with keeping the car on road, that lacks prediction capability, would only react when the car is already in the curve and loss of traction occurs.

The MPC is a widely used method for introducing prediction into multivariable control systems with constraints on states and control inputs. According to (Rossiter, 2003) p.6, the implementation of MPC is straightforward for variety of systems, because it handles

constraints systematically and it doesn't require any modifications to handle MIMO systems and dead time. MPC includes feed-forward control by implicitly utilizing future target information and is capable of handling challenging dynamics. The MPC algorithm uses an internal dynamic model of a process, a history of past control moves and an optimization cost function over the receding prediction horizon to calculate the optimum control moves. Often MPC is implemented for LTI state space models. Implementation for the Controller Auto-Regressive Moving-Average (CARIMA) models is also possible.

Conventionally, processes in industry have been using PID-controllers extensively. While PID-control is easy to implement due to its simplicity and universal understanding, conventional PID-control does not have the ability to include prediction into the control decision making. Most control solutions that are implemented by traditional PID-control can also be done with MPC. However, the prerequisite for MPC is acquisition of a robust dynamic process models, which is most often a linear empirical model obtained by system identification. Where as in PID-controller's case tuning is often in practice done experimentally in system commissioning phase. Ideally, the system commissioning does not need to spend time with MPC-controller tuning if the process model used has high enough fidelity to the real system.

The MPC has gained popularity due to its superior performance and improved profits in comparison to traditional PID-control and its ability solve complex problems. This is because the MPC can confidently reduce variance of an output and therefore process can be safely operated near constraints. Also, the minimization of the cost function ensures that consideration for economic aspects can be built inside the controller when the cost function is subjected to constraints, which reflect the boundaries set by economic and environmental aspects of system's operation. This gained ability to safely operate the system with optimal control when it is close to system boundary can result in increased output quantity, quality, minimized energy costs or environmental impact. The ability to incorporate constrains explicitly enables 'optimum' constrained performance as opposed to ad hoc fixes, like constraining the system with exterior constraints such as measurement range limits, as discussed by (Rossiter, 2003) p.5. Predictive aspect of MPC allows control to account for load changes, set-point changes and future references. Implementation of MPC can be easy for process industry, but tolerable control update

rate is relatively low, so implementation of MPC for fast processes should always consider time critical aspects of control action.

The optimization in a MPC is based on iterative, finite-horizon optimization of a plant model. In this thesis, the iteration part of the MPC algorithm is realized through quadratic cost function optimization with Quadratic Dynamic Matrix Control (QDMC). Minimization of other types of cost functions have been tried during development of MPC, but quadratic functions are by far most popular, because a quadratic function always has one global minimum. Finite-horizon prediction that ensures computation power required for calculation of an optimal control moves is not unlimited, however the prediction horizon should be long enough to capture the dynamics of the controlled system.

Because MPC algorithm is digital, it always uses discrete time approach. This mean the current plant state is sampled at the current time step and the cost-minimizing control strategy is computed by quadratic programming (QP) algorithm for the consequent steps until the prediction horizon is reached. Only the first step of the control strategy is implemented. After implementation, the plant state is sampled again. This introduces feedback into the control loop. Algorithm performs optimization again and control trajectory is updated. The prediction horizon shifts along, as the algorithm moves on to the next time step. Therefore, as stated in (D.Q. Mayne, 2000), p.1, the MPC is sometimes referred to as receding horizon control because the prediction horizon is always constant distance away from current time step.

4.1 The model predictive controller with QDMC algorithm

In this chapter I formulate MPC with QDMC algorithm for the target system. I divide the formulation into three sections, input data, offline computation, and on-line algorithm. This helps to draw the difference between necessary information required to begin the controller algorithm formulation, calculations that can be done before running the algorithm and steps of the online algorithm sequence. In figure 10, I have illustrated the functionality of the control chain from measurement to actuator of the freezer 1, as I have built it in the simulator in Matlab. This figure is applicable with decentralized MPC design, where each system has a separate LTI-system model, with a separate MPC-

controller application. I built both, a decentralised- and centralised MPC-controller applications in my Matlab simulation. In this thesis I discuss the centralised MPC application, where one LTI-system model contains all freezer and cooler models and one centralised MPC –controller optimises all the system outputs simultaneously. The benefit of this application is that it is possible to model the relationships between adjacent refrigerator system temperatures.

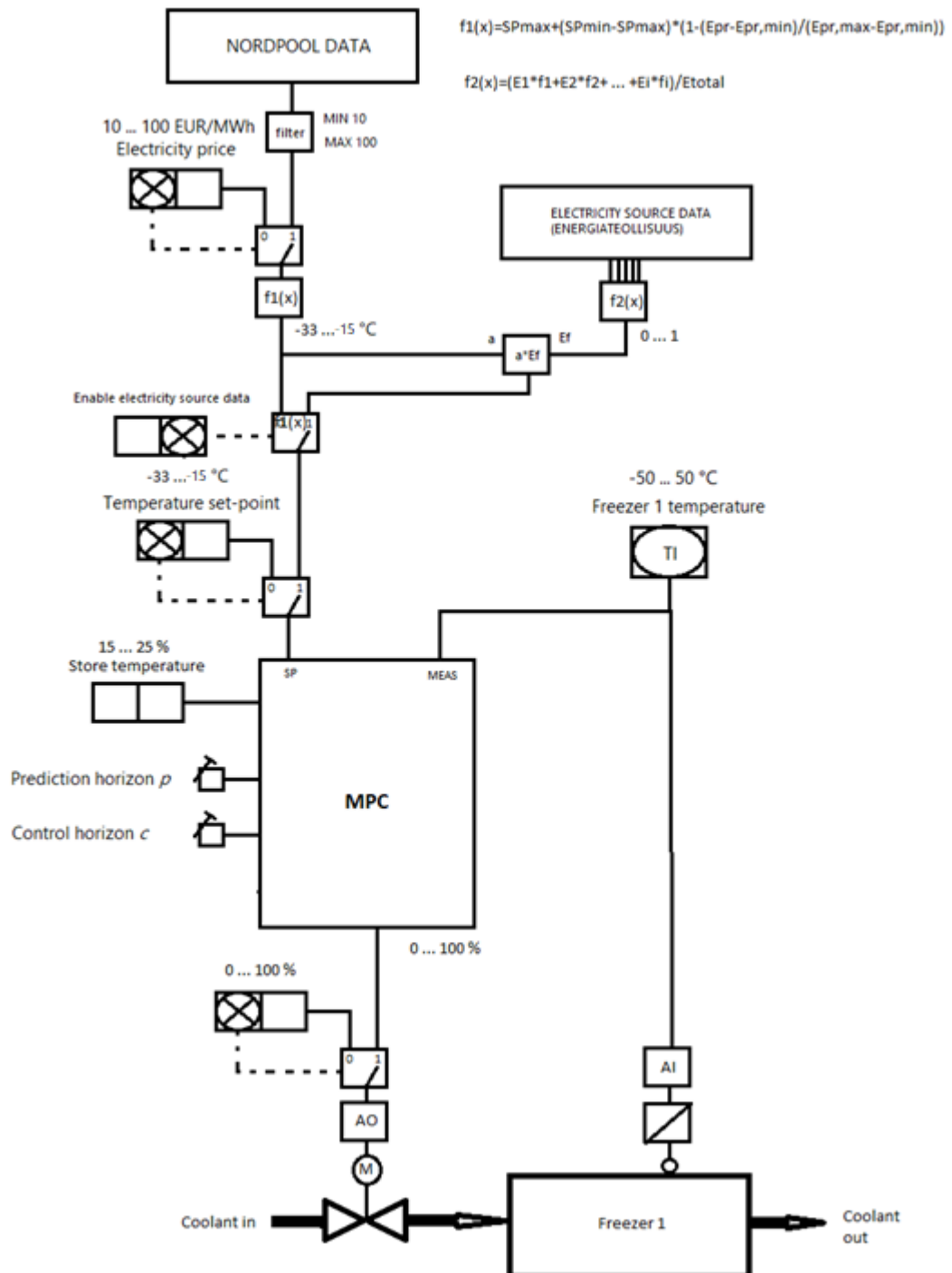


Figure 10. Functional diagram for freezer 1 decentralized MPC controller.

Figure 11 includes the explanations for drawing symbols for Figure 10.

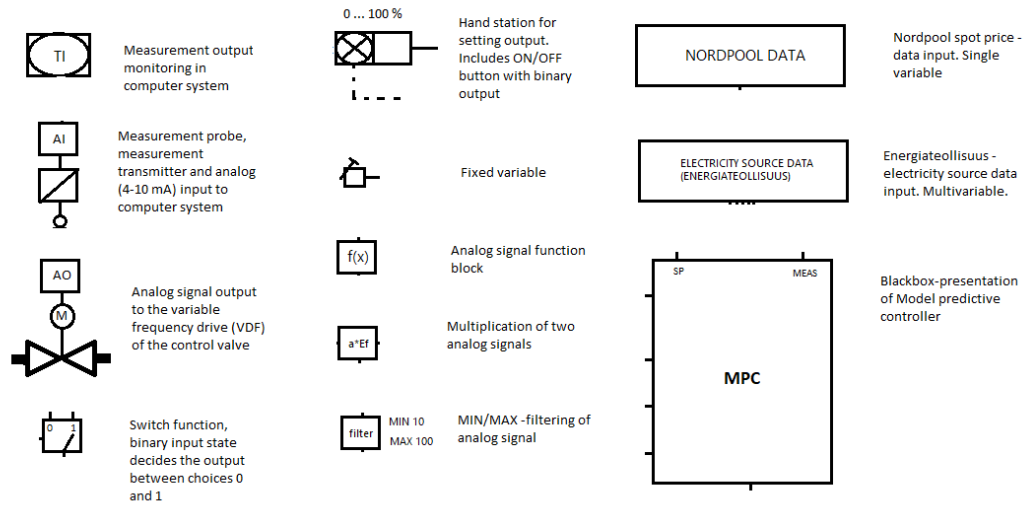


Figure 11. Explanations for drawing symbols for Figure 10.

4.1.1 Quadratic programming

To run the MPC-controller, I will formulate a QP for the case system. The objective function of QP is of the form:

$$\text{QP: } \min_{x \in \mathbb{R}^n} \frac{1}{2} x^T * H * x + h^T * x + (C), \text{ with the inputs } H, h.$$

Which is subjected to the constraints:

$$A_e * x = b_e$$

$$A_{ie} * x \leq b_{ie}$$

From the formulas (5) and (6) we can get the following constraint systems:

$$T_{air}^{min} \leq T_{air,k} \leq T_{air}^{max}$$

$$0 \leq \bar{u}_k \leq 1$$

Formulation of prediction matrices

First, I compute the matrixes M_x , M_u and M_T from the discrete system state-space formula (3):

$$x_{k+1} = Adx_k + Bd\bar{u}_k + Ddw_k$$

The matrix M_x represents the present state of the system, the matrix M_u includes the future predictions for the control variable and M_T is the recursive disturbance matrix. To find these matrixes, I use the one-step ahead prediction recursively to find an n-step ahead prediction:

$$\begin{aligned} x_{k+1} &= Adx_k + Bd\bar{u}_k + Ddw_k \\ x_{k+2} &= Adx_{k+1} + Bd\bar{u}_{k+1} + Ddw_{k+1} \\ x_{k+3} &= Adx_{k+2} + Bd\bar{u}_{k+2} + Ddw_{k+2} \\ x_{k+4} &= Adx_{k+3} + Bd\bar{u}_{k+3} + Ddw_{k+3} \end{aligned}$$

↓

$$\begin{aligned} x_{k+1} &= Adx_k + Bd\bar{u}_k + Ddw_k \\ x_{k+2} &= Ad[Adx_k + Bd\bar{u}_k + Ddw_k] + Bd\bar{u}_{k+1} + Ddw_{k+1} \\ x_{k+3} &= Ad(Ad[Adx_k + Bd\bar{u}_k + Ddw_k] + Bd\bar{u}_{k+1} + Ddw_{k+1}) + Bd\bar{u}_{k+2} + Ddw_{k+2} \\ x_{k+4} &= Ad[Ad(Ad[Adx_k + Bd\bar{u}_k + Ddw_k] + Bd\bar{u}_{k+1} + Ddw_{k+1}) + Bd\bar{u}_{k+2} + Ddw_{k+2}] + Bd\bar{u}_{k+3} + Ddw_{k+3} \end{aligned}$$

Expanding this out gives me:

$$\begin{aligned} x_{k+1} &= Adx_k + Bd\bar{u}_k + Ddw_k \\ x_{k+2} &= Ad^2x_k + AdBd\bar{u}_k + AdDdw_k + Bd\bar{u}_{k+1} + Ddw_{k+1} \\ x_{k+3} &= Ad^3x_k + Ad^2Bd\bar{u}_k + Ad^2Ddw_k + AdBd\bar{u}_{k+1} + AdDdw_{k+1} + Bd\bar{u}_{k+2} + Ddw_{k+2} \\ x_{k+4} &= Ad^4x_k + Ad^3Bd\bar{u}_k + Ad^3Ddw_k + Ad^2Bd\bar{u}_{k+1} + Ad^2Ddw_{k+1} + AdBd\bar{u}_{k+2} + AdDdw_{k+2} + Bd\bar{u}_{k+3} + Ddw_{k+3} \end{aligned}$$

Thus, the general expression of the n-step ahead prediction is:

$$\begin{aligned} x_{k+n} &= Ad^n x_k + Ad^{n-1} Bd\bar{u}_k + Ad^{n-1} Ddw_k + Ad^{n-2} Bd\bar{u}_{k+1} + Ad^{n-2} Ddw_{k+1} + \dots \\ &\quad + AdBd\bar{u}_{k+n-2} + AdDdw_{k+n-2} + Bd\bar{u}_{k+n-1} + Ddw_{k+n-1} \end{aligned}$$

Therefore, n-step ahead prediction at time instant k is of the form:

$$\vec{x}_{k+1} = \begin{bmatrix} x_{k+1|k} \\ x_{k+2|k} \\ \vdots \\ x_{k+n|k} \end{bmatrix}$$

Expanding this gives:

$$\vec{x}_{k+1} = \begin{bmatrix} Adx_k + Bd\bar{u}_k + Ddw_k \\ Ad^2x_k + AdBd\bar{u}_{k|k} + AdDdw_{k|k} + Bd\bar{u}_{k+1|k} + Ddw_{k+1|k} \\ \vdots \\ Ad^n x_k + Ad^{n-1}Bd\bar{u}_{k|k} + Ad^{n-1}Ddw_{k|k} + Ad^{n-2}Bd\bar{u}_{k+1|k} + Ad^{n-2}Ddw_{k+1|k} + \dots \\ + AdBd\bar{u}_{k+n-2|k} + AdDdw_{k+n-2|k} + Bd\bar{u}_{k+n-1|k} + Ddw_{k+n-1|k} \end{bmatrix}$$

Separating this into past and decision variables gives:

$$\begin{aligned} \vec{x}_{k+1} &= \begin{bmatrix} Adx_k \\ Ad^2x_k \\ \vdots \\ Ad^n x_k \end{bmatrix} + \begin{bmatrix} Bd\bar{u}_k \\ AdBd\bar{u}_{k|k} + Bd\bar{u}_{k+1|k} \\ \vdots \\ Ad^{n-1}Bd\bar{u}_{k|k} + Ad^{n-2}Bd\bar{u}_{k+1|k} + \dots \\ + AdBd\bar{u}_{k+n-2|k} + Bd\bar{u}_{k+n-1|k} \end{bmatrix} + \begin{bmatrix} Ddw_k \\ AdDdw_{k|k} + Ddw_{k+1|k} \\ \vdots \\ Ad^{n-1}Ddw_{k|k} + Ad^{n-2}Ddw_{k+1|k} + \dots \\ + AdDdw_{k+n-2|k} + Ddw_{k+n-1|k} \end{bmatrix} \\ &= \underbrace{\begin{bmatrix} Ad \\ Ad^2 \\ \vdots \\ Ad^n \end{bmatrix}}_{M_x} x_k + \underbrace{\begin{bmatrix} Bd & 0 & \dots & 0 \\ AdBd & Bd & \dots & 0 \\ \vdots & \vdots & \ddots & \vdots \\ Ad^{n-1}Bd & Ad^{n-2}Bd & \dots & Bd \end{bmatrix}}_{M_u} \underbrace{\begin{bmatrix} \bar{u}_{k|k} \\ \bar{u}_{k+1|k} \\ \vdots \\ \bar{u}_{k+n-1|k} \end{bmatrix}}_{\vec{u}_k} + \underbrace{\begin{bmatrix} Dd & 0 & \dots & 0 \\ AdDd & Dd & \dots & 0 \\ \vdots & \vdots & \ddots & \vdots \\ Ad^{n-1}Dd & Ad^{n-2}Dd & \dots & Dd \end{bmatrix}}_{M_T} \underbrace{\begin{bmatrix} w_{k|k} \\ w_{k+1|k} \\ \vdots \\ w_{k+n-1|k} \end{bmatrix}}_{\vec{w}_k} \end{aligned}$$

Finally, the prediction matrices for the system matrices are computed in the form:

$$\vec{x}_{k+1} = \underbrace{M_x x_k}_{\text{present}} + \underbrace{M_u \vec{u}_k + M_T \vec{w}_k}_{\text{future}} \quad (7)$$

(9) can be rearranged as:

$$\begin{bmatrix} x_{k+1} \\ x_{k+2} \\ x_{k+3} \\ \vdots \end{bmatrix} = M_u * \bar{u}_t + b_t, \quad (8)$$

where

$$b_t = M_x * x_k + M_T * w_k.$$

System constraints

The constraint system for the valve openings can be formulated as:

$$\begin{bmatrix} 0 \\ 0 \\ 0 \\ \vdots \end{bmatrix} \leq \begin{bmatrix} \bar{u}_k \\ \bar{u}_{k+1} \\ \bar{u}_{k+2} \\ \vdots \end{bmatrix} \leq \begin{bmatrix} 1 \\ 1 \\ 1 \\ \vdots \end{bmatrix},$$

which can be written as:

$$u_t^{min} \leq \bar{u}_t \leq u_t^{max}.$$

The vectors u_t^{min} and u_t^{max} can be set as QP's lower- and upper boundary for the controlled value, the valve opening, in the Matlab.

Next, I formulate the boundaries for the refrigerator system air temperature. According to (1) refrigerator system consists of two temperatures, the refrigerator air temperature and refrigerated goods temperature. Example of this is:

$$x_k = \begin{bmatrix} T_{air,k} \\ T_{g,k} \end{bmatrix}$$

Because refrigerated goods temperature always follows the refrigerator air temperature, setting up constraints for only the air temperature will work to also constraint the goods temperature. Refrigerator air temperature can be separated from the system matrix by multiplying with the matrix e^T :

$$\underbrace{[1 \ 0]}_{e^T} x_k = T_{air,k}$$

$$e^T * x_k = T_{air,k}$$

This can be generalised for all time steps as follows:

$$\underbrace{\begin{bmatrix} e^T & 0 & 0 & \cdots \\ 0 & e^T & 0 & \cdots \\ 0 & 0 & e^T & \cdots \\ \vdots & \vdots & \vdots & \ddots \end{bmatrix}}_P \begin{bmatrix} x_{k+1} \\ x_{k+2} \\ x_{k+3} \\ \vdots \end{bmatrix} = \begin{bmatrix} T_{air,k} \\ T_{air,k+1} \\ T_{air,k+2} \\ \vdots \end{bmatrix}$$

From combining this with the formula (11) gives:

$$\begin{bmatrix} x_{k+1} \\ x_{k+2} \\ x_{k+3} \\ \vdots \end{bmatrix} = M_u * \bar{u}_t + b_t \rightarrow \begin{bmatrix} T_{air,k} \\ T_{air,k+1} \\ T_{air,k+2} \\ \vdots \end{bmatrix} = P * M_u * \bar{u}_t + P * b_t$$

Therefore, setting the system between refrigerator air temperature boundaries gives:

$$\underbrace{\begin{bmatrix} T_{air,k}^{min} \\ T_{air,k+1}^{min} \\ T_{air,k+2}^{min} \\ \vdots \end{bmatrix}}_{T_t^{min}} \leq \underbrace{P * M_u}_{A_P} * \bar{u}_t + P * b_t \leq \underbrace{\begin{bmatrix} T_{air,k}^{max} \\ T_{air,k+1}^{max} \\ T_{air,k+2}^{max} \\ \vdots \end{bmatrix}}_{T_t^{max}}$$

This can be split into two formulas:

$$A_P * \bar{u}_t \leq T_t^{max} - P * b_t$$

$$-A_P * \bar{u}_t \leq -T_t^{min} + P * b_t$$

These, in turn, can be combined into matrices A_{ieq} and b_{ieq} :

$$A_{ieq} = \begin{bmatrix} A_P \\ -A_P \end{bmatrix}, b_{ieq} = \begin{bmatrix} T_t^{max} - P * b_t \\ -T_t^{min} + P * b_t \end{bmatrix},$$

which can be inputs for Matlab's QP -function, where the input matrices for constraints are required be of the form:

$$A_{ieq} * \bar{u}_t \leq b_{ieq}$$

Objective function formulation

The target of the objective function formulation is to minimise the differential between temperature reference and system temperature over all time steps. This can be written as a form as:

$$\lim_{k \rightarrow \infty} (T^{ref} - T_{air,k}) = 0$$

The e_k is the steady-state error at time step k . With infinite time horizon the objective function can be written as:

$$\underbrace{\begin{bmatrix} e_k \\ e_{k+1} \\ e_{k+2} \\ \vdots \end{bmatrix}}_{e_t} = \begin{bmatrix} T^{ref} - T_{air,k} \\ T^{ref} - T_{air,k+1} \\ T^{ref} - T_{air,k+2} \\ \vdots \end{bmatrix} = \underbrace{\begin{bmatrix} T^{ref} \\ T^{ref} \\ T^{ref} \\ \vdots \end{bmatrix}}_{T_t^{ref}} - \underbrace{\begin{bmatrix} T_{air,k} \\ T_{air,k+1} \\ T_{air,k+2} \\ \vdots \end{bmatrix}}_{P * M_u * \bar{u}_t + P * b_t}$$

The objective of QP is to minimize the length of the vector e_t . The e_t vector contains all the steady-state errors on all time steps until the QP reaches its objective.

As e_t is symmetric positive-definite matrix, the length of e_t is minimized with least-squares:

$$e_t = \|e_t\| = \sqrt{e_t^T * e_t} \rightarrow \min(e_t^T * e_t),$$

where

$$e_t = T_t^{ref} - P * M_u * \bar{u}_t + P * b_t,$$

which can be written as

$$e_t = -A_p * \bar{u}_t + e_o,$$

where

$$e_o = T_t^{ref} - P * b_t.$$

Expanding this out gives:

$$\begin{aligned}
e_t^T * e_t &= (e_0^T - \bar{u}_t^T * A_p^T)(e_o - A_p * \bar{u}_t) \\
&= e_0^T * e_o - e_0^T * A_p * \bar{u}_t - \bar{u}_t^T * A_p^T * e_o + \bar{u}_t^T * A_p^T * A_p * \bar{u}_t - e_0^T * A_p \\
&\quad * \bar{u}_t \\
&= \bar{u}_t^T * A_p^T * A_p * \bar{u}_t - 2 * e_0^T * A_p * \bar{u}_t + e_0^T * e_o \\
&= \frac{1}{2} \bar{u}_t^T \underbrace{2 * A_p^T * A_p}_H * \bar{u}_t + \underbrace{(-2 * e_0^T * A_p)}_{h^T} * \bar{u}_t + \dots
\end{aligned}$$

Now H and h^T are in a form that can be input into Matlab's QP.

4.1.2 The MPC-control simulator algorithm

The simulator algorithm can be thought to include three parts, input data, offline computations, and on-line computations.

Input data

To construct the QDMC controller the following are needed as input data:

- According to (Tenhomaa, 2016), the model for freezer system is the following discrete LTI state-space model of the formula (3):

$$x_{k+1}(t) = Ad * x(t) + Bd * \tilde{u}(t) + Dd * T_{env}(t),$$

These matrices are discretized by using the sampling time of 1 minute.

- Limit values for process. Valve maximum and minimum openings, which are the manipulated variables, and refrigerator system maximum and minimum temperatures, which are controlled variables.
- *Nordpool* spot price data
- Electricity source data from *Energiategollisuus*
- Initial values for refrigerator system air and goods temperatures, valve openings, measurement disturbances, which are in this case the ambient temperatures of

shop floor and storage area, and system set-point temperatures, which are different for freezers and coolers.

- Prediction horizon p
- Control horizon c
-

Offline computation

The MPC includes components, which remain unchanged during the runtime of the controller. Therefore, calculating these offline before implementation saves computational complexity. Offline calculations the prediction,

$$\vec{x}_{k+1} = \underbrace{P_x x_k}_{\text{present}} + \underbrace{H_x \vec{u}_k + L_x \vec{w}_k}_{\text{future}}, \quad (7)$$

valve opening limits, and A_{ieq} ,

$$A_{ieq} = \begin{bmatrix} A_p \\ -A_p \end{bmatrix}, \quad (8)$$

the refrigerator system temperature limits. b_{ieq} must be calculated again at every time step before running the QP.

On-line algorithm

1. First, the algorithm moves to the next sample index $k := k + 1$. Initial state of the system is obtained by using initial values on the first computation round.
2. Now the online algorithm computes the refrigerator system air temperature set-point depending, is the set-point calculation conditioned on *Nordpool*, and if it is conditioned on *Energiategollisuus* –electricity source data.
3. The algorithm checks if disturbance is to be added into the system simulation.
4. The algorithm checks if noise $d(k)$ is to be added into the system simulation.

5. MPC control is computed if controller is switched on.

1. The control decisions are updated by using a QP to calculate the free response prediction. QP with by minimizing the target function:

$$\text{QP: } \min_{x \in \mathbb{R}^n} \frac{1}{2} x^T * H * x + h^T * x + (C), \text{ with the inputs H, h.}$$

Which is subjected to the constraints:

$$Ae * x = be$$

$$Aie * x \leq bie$$

From the formulas (5) and (6) we can get the following constraint systems:

$$T_{air}^{min} \leq T_{air,k} \leq T_{air}^{max}$$

$$0 \leq \bar{u}_k \leq 1$$

2. The model and process are simulated for current time step to observe the outcome of current system transient.
6. Control output is updated using new computed control decisions.
7. The system state is plotted to monitor feedback of the real time simulation. After plotting, the algorithm loops back to Step 1.

5 DESCRIPTION OF MATLAB MODEL

For the purposes of this thesis, have modelled the refrigerators of the CO₂ vapour compression cycle of Tuira supermarket by building a simulator in Matlab. The purpose of the simulator application is to compose an interactive demonstration of the real-life vapour compression cycle process, which includes 6 freezers and 14 refrigerators. The figure 12 illustrates the shop layout window where the freezers and coolers have been positioned according the shop floor plan.

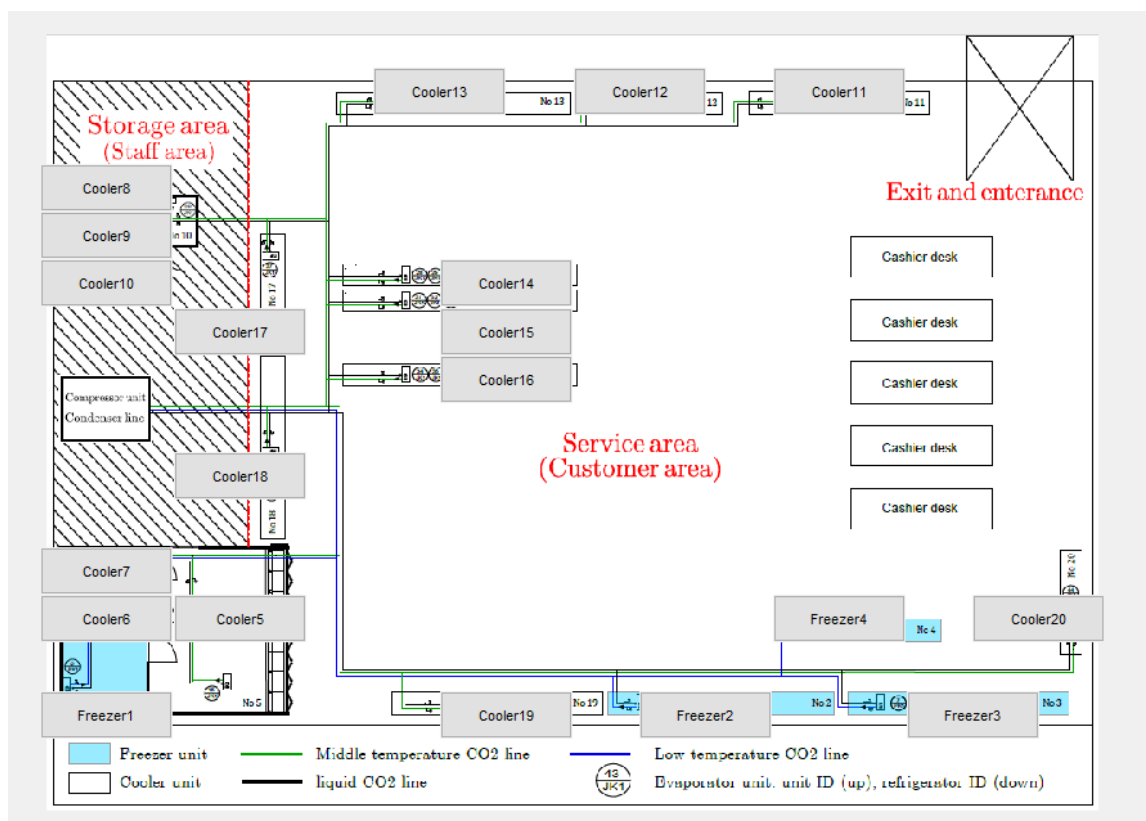


Figure 12. The layout of S-market Tuira in modelling application.

Freezers and coolers in storage area and customer area have slightly different dynamics due to difference in ambient temperature and dimensions and structure of equipment. These dynamics are captured in the system model that was formulated in (Tenhoma, 2016), p.23.

Clicking the press buttons for coolers or refrigerators on the shop floor window switches which system the simulation window, shown in figure 13, illustrates. The simulation window, figure 13, shows the simulation interface of the chosen refrigeration system. The simulation results are plotted in real time with X-axis of plot representing one simulation minute per each real time minute. In Figure 13, at the Freezer simulation axis, Y-axis of the plot visualizes the temperature response of the simulation. In this axis we plot current simulated refrigerator system air (red line) and goods (green line) temperatures and MPC-controller set-point (blue line). In Valve status -axis, Y-axis represents valve opening degree, and here we plot valve opening and minimum and maximum valve opening degree. In Electricity price axis, Y-axis represents current electricity spot price (€/MWh). Here we plot current electricity price, which is used for set-point calculation of MPC-controller and example *Nordpool* spot price data, which can be fed to set-point calculation of the MPC. Additionally, the calculated renewable energy proportion of the power grid is displayed at the Renewable portion -axis, which is also used for MPC-controller set-point selection. The simulation responds to parameter changes in real time and the user interface allows user to experiment with different parameters to realize the effect of parameter changes. Because the prediction horizon is 15 minutes, we can see at around 42-minute simulation step that the controller sees the upcoming set-point change and begins to respond to it accordingly. The set-point changes are scheduled according to known data, so the controller has the ability anticipate set-point changes up to the length of prediction horizon, and the QP cost function calculates a trajectory that minimizes the difference between set-point- and system temperatures for this duration.

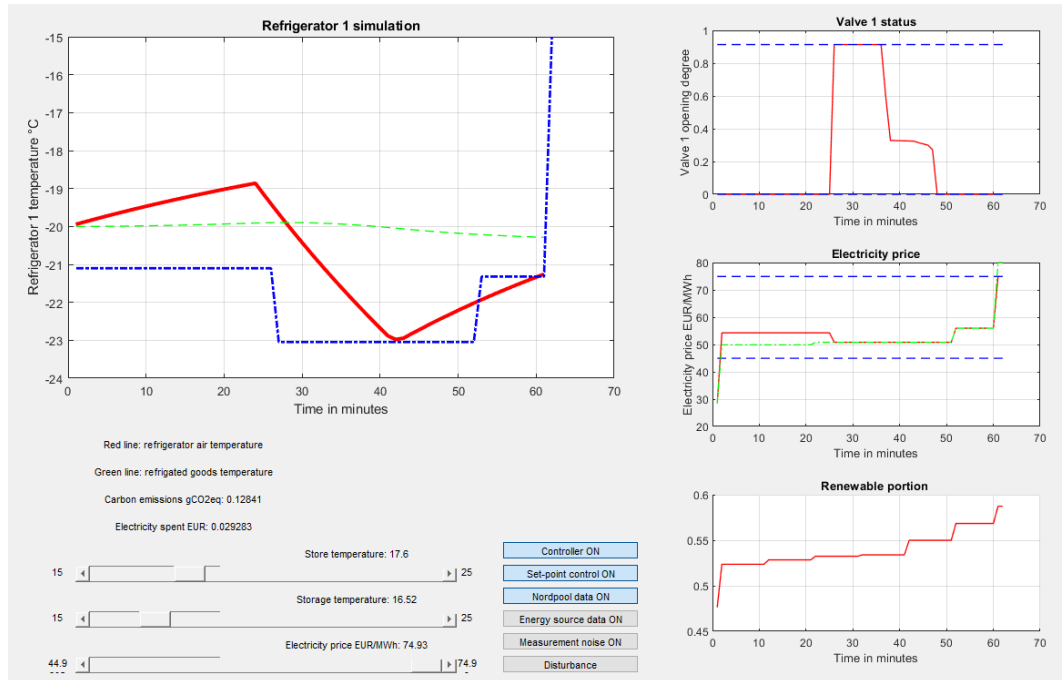


Figure 13. Simulation window for freezer 1.

The simulation window has levers for shop floor- and storage temperatures, which are known measurable disturbances. These parameters affect the refrigerator system modelling and their effect on the refrigerator system temperatures can be illustrated by changing the values. The magnitude of the effect of the shop temperatures are slightly different for different freezers and coolers. In practice the different refrigerators are affected by shop temperature differently depending on whether they are placed on storage or service area, because the storage temperature is often lower than shop floor temperature.

The MPC controller can be switched on and off with a toggle button. When MPC controller is switched on, the valve opening control is taken over by the MPC controller and valve openings start following optimal control moves that the MPC calculates according to system state, system model and set-point, which can be controlled from its own slider bar. Pressing Set-point control ON -toggle button will make set-point of MPC-controller follow electricity price (€/MWh), which has its own slider bar in turn. *Nordpool* spot price -toggle button will make electricity price follow *Nordpool* spot price data. The data used in this simulation is the Finnish electricity spot price data onwards from January

of 2019. The Energy source data ON -button enables the renewable energy proportion of the power grid to be used in the refrigerator temperature set-point selection.

Additionally, user interface includes a toggle button for adding measurement noise to system, which only applies to system, when MPC-controller is enabled, because measurement does not affect simulated system state, unless the measurement noise is fed to the controller. Without control, measurement noise will not be fed back into the system. User interface has a push button to insert disturbance into the system. This could correspond to, for example, opening the freezer door, where outside air mixes with inside air of the freezer and therefore quickly rising the freezer temperature.

Figure 14 is the Overview and control –window of the simulator. This window displays the set-point temperatures of the refrigerator systems, all the valve openings corresponding to different systems and the refrigerator system air temperatures. The set-point temperatures can be manually changed here, if Set-point control ON –button is not pressed in the simulation window, figure 13. Also, the valve openings can be changed manually, if the MPC controller is not enabled likewise. Each refrigerator system can have one to four control valve openings that can be given values between 0 and 1. This represents the degree of thermostat valve opening, where 0 represents completely closed and 1 fully open. Maximum valve openings are limited to less than 100% open, and these have been considered as a limitation for valve opening degrees inside the Matlab algorithm and this is not shown outwardly.

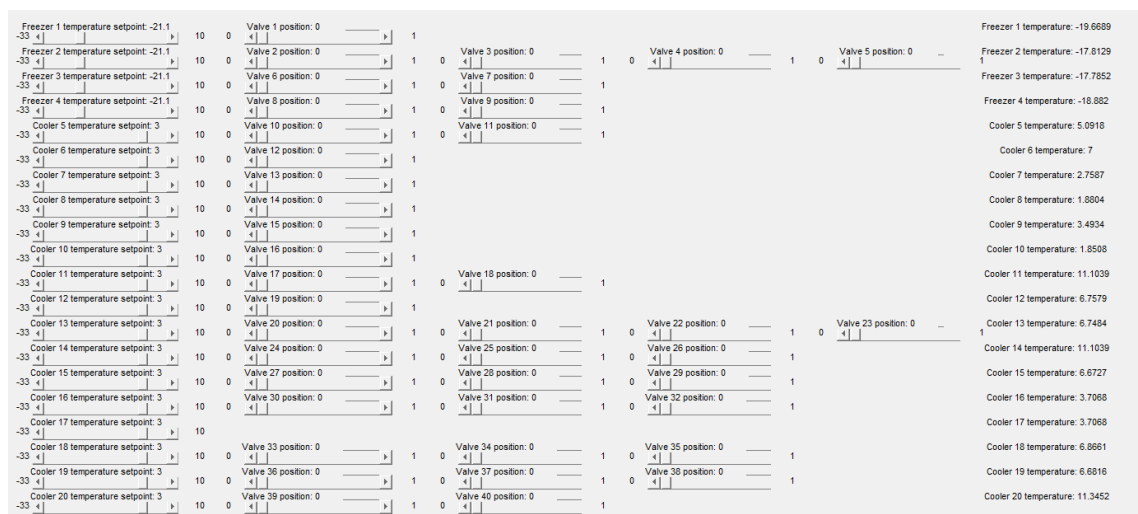


Figure 14. Overview and control window for the Matlab simulator.

In figure 15, I have conducted step-response test with the simulator to change in the temperature set-point of freezer 1. Here we can see the refrigerator air temperature (red line) start following the air set-point temperature (blue line) right after the MPC-controller is switched on around the time step corresponding to 7 minutes. The refrigerated goods temperature (green line) can be seen lagging behind the air temperature. The refrigerated goods temperature would only reach the refrigerator air temperature after several hours of constant air temperature.

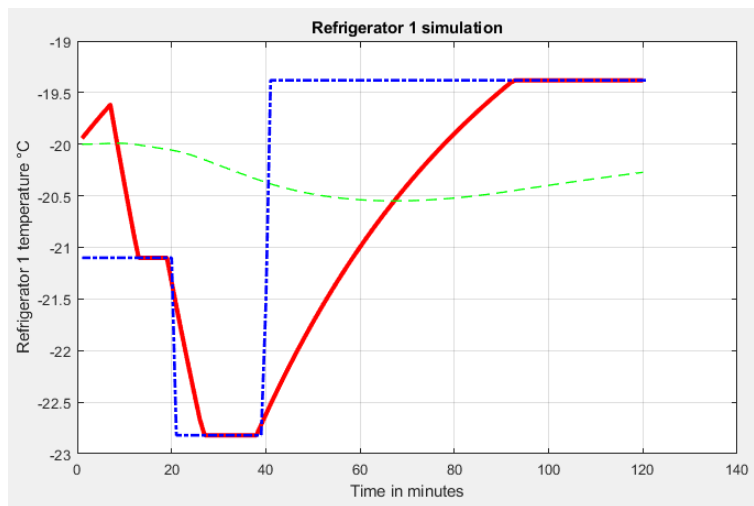


Figure 15. The Step-response test with the freezer system 1.

In the figure 16, in turn, we can observe that the control valve responds to a freezing event by opening completely, until the set-point temperature is nearly reached, at which point the control valve begins closing up to an valve opening, where the system maintains steady-state. (The valve complete valve opening doesn't show up in this graph when the MPC controller is turned on) Conversely, the rise of the set-point closes the control valve completely, until system is near the set-point temperature, at which point the valve opening settles up to the steady-state valve opening. The controller has a good capability of controlling the system and the control is optimal. The control response does not exhibit overshoot and the rising time is minimum within given boundaries and control settles immediately to the steady state, without any oscillation. The control is arguably optimal within the given system model and its constraints. If the control behaviour differentiates

in real-life application from the simulated model control results, it would be due to dynamics not included in the system model or possible discrepancies between the system model and the real-life system or system constraints that are not accurate or not considered in the simulation.

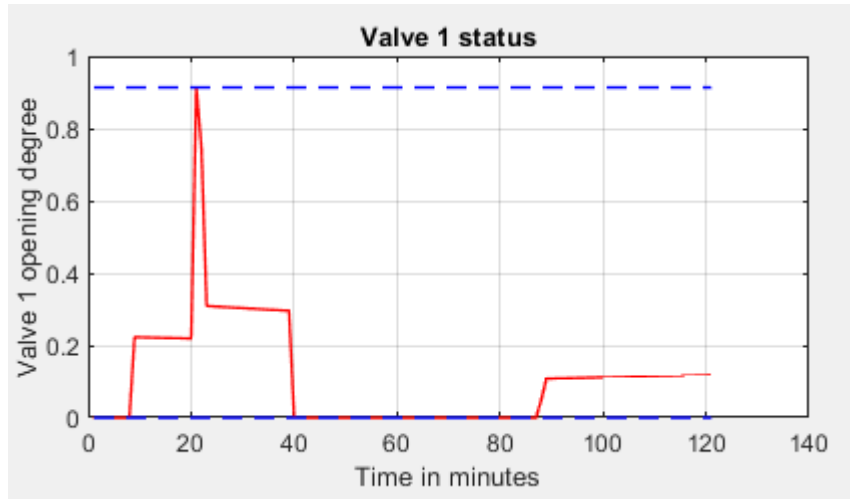


Figure 16. Valve-opening for freezer 1 corresponding to Figure 15 step-response test.

6 TEMPERATURE SET-POINT SELECTION STRATEGIES

6.1 Nord pool spot price -based temperature set-point selection

Nord Pool AS is a European power exchange that trades power across Europe. Nord Pool offers day-ahead and intraday trading, clearing and settlement, data, compliance, and consultancy services. The markets that Nord Pool operates in are Norway, Denmark, Sweden, Finland, Estonia Latvia Lithuania, Germany, The Netherlands, Belgium, Austria, Luxembourg, France, and the United Kingdom. In this thesis work we are interested in electricity price data from Finland. Figure 17 illustrates electricity price fluctuation of *Nordpool* spot price in January of 2019. I use this data in simulations with the intent of benchmarking different set-point control strategies.

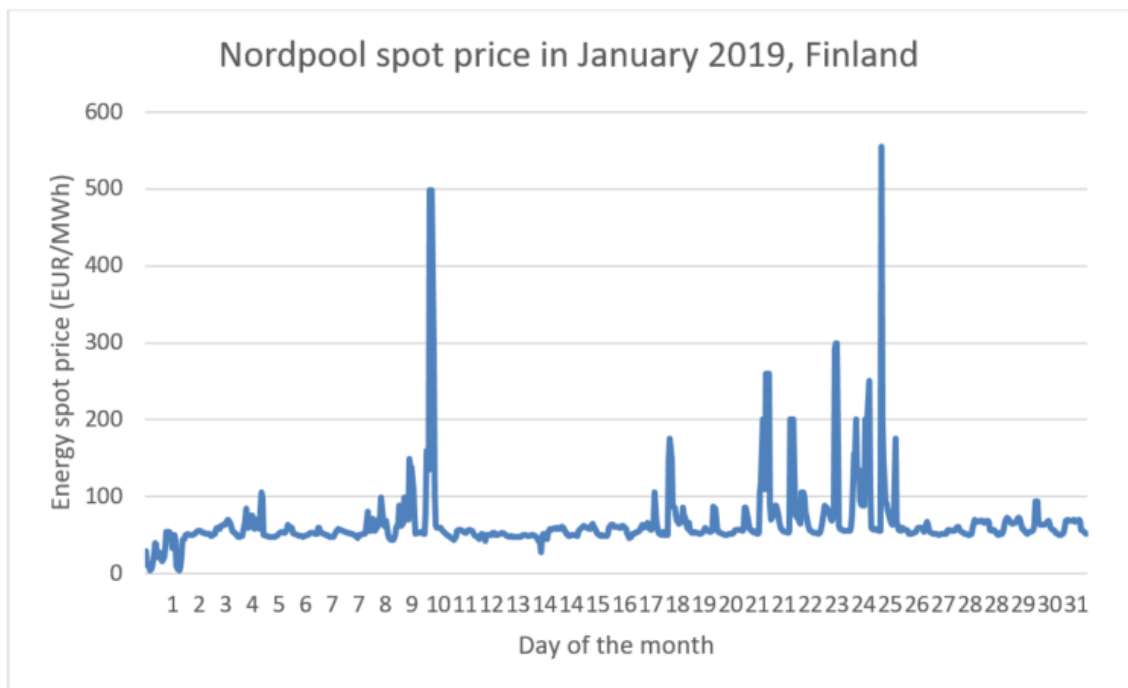


Figure 17. *Nordpool* spot price fluctuation in January 2019. (Nordpool, 2019)

The *Nordpool* spot pricing reflects the hourly availability of power grid electricity. As we know, the renewable energy generation does not convey any fuel costs and does not convey any additional production costs, once the infrastructure is in place. Therefore, it is intuitive, that the peak renewable energy generation would be reflected in electric

power wholesale market prices, such as *Nordpool* spot price, as spot price reduction. In German energy market analysis done by (Marius Dillig, 2016), in abundance of any renewable power, the German market price for electricity would have increased by astonishingly high amount of 0,0529 €/kWh during the period of 2011 to 2013. Due to this, the German power consumers saved nearly 30 billion euros during this period thanks to renewable power utilization. Now, this presents a bigger opportunity for singular power consumers for higher savings by scheduling their consumption complement the intermittent nature of renewable power through the means of DR.

Keeping up with peak power demand is expensive and building the infrastructure is even more so. This is reflected in *Nordpool* spot price as price peaks. Energy sinks are mean to mitigate peak power demand, by reducing power consumption during peak power demand. This is my justification for implementing a spot price data –based temperature set-point control strategy in my refrigeration system simulator to investigate its viability as a cost and carbon emission saving method. My intention is to find out if the online simulator can visualise the energy sink capabilities of a refrigerator system.

The basis of my control strategy is to over freeze our frozen goods during periods of high renewable power generation and decrease power consumption during hours, when regional power consumption is high, but renewable energy production goes down. In this strategy I implement this as an incentive scheme, where refrigerator set-point follows the electricity price. The correlation between electricity price and freezer set-point, in the case of freezer control simulator, is chosen to be linear over the set-point range, because of simplicity and ease of visualization. Set point is -33 °C when electricity price is at minimum of 45,0 €/MWh and -15 °C at the price maximum of 75,0 €/MWh, so we will not allow the refrigerates to thaw. Formula for correlation is:

$$SP = SP_{max} + (SP_{min} - SP_{max}) * \left(1 - \frac{E_{pr} - E_{pr,min}}{E_{pr,max} - E_{pr,min}}\right), \quad (9)$$

where

SP = refrigerator system set-point

SP_{max} = refrigerator system lowest allowed temperature, in case of a freezer -15 °C

SP_{min} = refrigerator system lowest allowed temperature, in case of a freezer -33°C

E_{pr} = Electricity price

$E_{pr,min}$ = Electricity price corresponding to lowest allowed refrigerator temperature

$E_{pr,max}$ = Electricity price corresponding to highest allowed refrigerator temperature.

I selected minimum price limit $E_{pr,min}$ by calculating 5 % percentile of 1000 hours of *Nordpool* spot price -data. This means that 95 % of dataset values are higher than 45,0 €/MWh. Similarly, Maximum price limit, $E_{pr,max}$, is 90 % percentile of the same dataset, and therefore 90% of dataset values are smaller than 75,0 €/MWh. Minimum and maximum range selection has a significant effect to optimal ability for cooling sink capability in the chosen set-point control strategy. Too wide set-point range will not capture the full benefit of periodic nature of daily electricity price fluctuation, because the set-point differences between high and low price periods are too narrow, which leads to low amount of energy storing capacity utilization. Too narrow set-point range, on other hand, can differentiate the choice between day and night electricity, by flipping the freezer set-point between the extremes, but will not capture the full benefit of price curve dynamic. This can, for example, lead us to over-freeze our freezer before price reached the periodical low point. In this case, higher savings could be achieved by waiting a bit longer for an electricity price plummet before lowering the set-point all the way down.

Figure 7.1 has a plot of *Nordpool* spot price data of January 2019. Here we can see that peaks can be extreme, at up to 500 €/MWh at the most expensive hours. However, on normal days the prices stay in the range of 40 to 65 €/MWh, lowest being after midnight and highest on the evening. This periodical nature of the spot pricing can help us prepare for the peak consumption by lowering the set-point of our freezer during night hours, where the spot price is low.

6.2 Power grid composition -based set-point temperature selection

Using electricity spot price forecasts are ideal as a money saving strategy for an individual consumer. However, as explained (Eric S. Hittinger, 2015), according to (Laura M.

Arciniegas, 2018), p. 2, merely basing the control strategy on electricity spot price does not always lead to desirable carbon footprint elimination outcomes. In California, the Tesla Powerwalls have been widely implemented as a mean of domestic power storage. However, as (Eric S. Hittinger, 2015), according to (Laura M. Arciniegas, 2018), p. 2 pointed out, the early proliferation of household energy storage only worked to further increase the total carbon emissions. If the only metric is financial benefit for the battery owner, the batteries tend to charge with cheap, dirty power at night and discharge during the day for peak reduction, and this ends up increasing the total emissions. One possible explanation for how the energy storages can end up fulling with 'dirty' electricity is a positive feedback loop, where a Peaker plant starts burning cheap gas, which ends up lowering the electricity spot price. Energy storage reacts to the low spot price by increasing consumption by storing more electricity. Peaker plants, in turn, ramp energy production even further due to the increased energy demand. The loop would go on until all energy storage capacity is full.

Energy market spot price forecasts may not be a completely wrong choice to account for in the decision making within every power system in the world. However, in areas where electricity spot prices do not account for carbon footprint of the electricity, the control algorithms must include more variables into decision making. Only considering spot price minimizes the price of electricity for the customer, but it does not necessarily reach the best solution in terms of emission reduction, because electricity price does not by itself consider how it is produced. Increasing the output of coal power plant can also drive the spot price down when the coal price is low. Therefore, our algorithm needs to know, whether the electricity is clean or dirty. The significance of this is pointed in the previously mentioned (Laura M. Arciniegas, 2018) p.1, where it was stated that CO₂ emission related to battery storage of electricity could be decreased by (25-50%) with little cost penalty (1-5%), when we move away from fully following spot prices to a strategy that also takes into account the carbon footprint of the electricity currently in the power grid. The climate impact reducing algorithms always induce a small penalty for the consumer price, but this is always necessary, because not focusing on climate impact will render energy storage be counterproductive to its goal of proliferating the renewable energy penetration of the power grid.

The solution is to develop smarter algorithms, which can consider how the electricity is produced along with the electricity price. I want to consider an approach, where we correct the set-point with a factor, which corresponds to the current carbon footprint of the power grid.

In my simulations, I use the power production data for the power grid in Finland provided by *Energiategollisuus*. By assigning a carbon footprint factor for each type of energy production method, which corresponds to climate change inducing emissions produces per unit of energy, and dividing by total energy production, I will calculate a factor, which can be used to roughly evaluate the feasibility of DR through energy storage at given time. Life-cycle assessments of any given energy source can be used to improve the estimates of their climate impact. I expect this approach to give the best possible carbon footprint estimation method.

Problem with implementing this in real-life is that real-time data of the power grid's electricity source composition may not be obtainable. However, this can be used to benchmark the climate impact reducing energy storage algorithms that base their decision making on other available data for carbon footprint estimation to properly contextualize the electricity spot price data. Useful information for determining whether the electricity is clean or dirty can be obtained by monitoring variables, such as weather data, fuel prices, wind, etc. in addition to spot price data.

For temperature set-point selection strategy, which is on carbon footprint of the power grid electricity source composition, I propose the formulation:

$$SP = SP_{max} + (SP_{min} - SP_{max}) * (1 - E_f), \quad (10)$$

where E_f is between 0 and 1 and corresponds to the renewable portion of the electricity in the power grid. Here 0 means that the electricity is completely produced by carbon emission causing means and 1 corresponds to completely carbon neutral power. An E_f -factor, that is close to one means that electricity in the power grid is increasingly carbon free and energy storage is encouraged. Conversely, E_f factor close to zero means the electricity in the grid is produced by burning fossil fuels, and stored energy is

recommended to be discharged to prevent further emissions. I formulated a simple proposal for how renewable portion E_f could be obtained:

$$E_f = \frac{E_1 f_1 + E_2 f_2 + \dots + E_i f_i}{E_{total}}, \quad (11)$$

where E_{total} is the power grid's total energy capacity at the moment. The power load portions of different electricity sources E_i are multiplied by the factor f_i and summed together. The factor f_i represents carbon footprint of each electricity source. Obtaining the carbon footprint proportion of each energy source requires life-cycle assessments of the whole source, which would include emissions caused by building of the infrastructure, fuel acquirement, fuel combustion, maintenance, decommissioning, etc.

Life-time assessments different power sources has been done by (Pehl, 2017) p.941. This study finds that each kilowatt hour of electricity generated over the lifetime of a nuclear plant has an emissions footprint of 4 grams of CO₂ equivalent (gCO₂eq/kWh). The footprint of solar comes in at 6 gCO₂eq/kWh and wind is also 4 gCO₂eq/kWh. In contrast, coal CCS (109 gCO₂eq/kWh), gas CCS (78 gCO₂eq/kWh), hydro (97 gCO₂eq/kWh) and bioenergy (98 gCO₂eq/kWh) have relatively high emissions, compared to a global average target for a 2°C world of 15gCO₂e/kWh in 2050. Here I find the high footprint of hydropower highly surprising. The study by (Pehl, 2017) p.942 further explains that footprint for hydro is highly variable. The high lifecycle emissions largely due to poorly chosen locations where the building the dam has flooded forests, which has led to the rotting organic matter emitting methane, which is a highly potent greenhouse gas. This means that construction of hydropower should be avoided in warm regions with large variations in water level, where wide expanses of forest can get flooded. My understanding is that the hydropower is not built by flooding forests in Finland, and thus I use more carbon neutral life-cycle assessment values in my simulations. Even beyond hydro power, we should have use local emission footprint data for the purposes of controlling energy sinks in Finland, if available.

During simulations with the electricity source data, I omitted the electricity import and export data because life-cycle analysis for this electricity's carbon footprint would be difficult to assess. However, for the sake of this test I find omitting this information acceptable. The difference this makes in renewable portion calculation is that I remove

related terms from nominator and the corresponding capacity portions from E_{total} in denominator.

The carbon footprint factors f_i will need to be scaled between 0 and 1 for the purposes of this formulation, where 0 corresponds to biggest global warming impact and 1 correspond to no global warming impact. I propose that CO₂ equivalent values for each electricity source can be scale between 0 and 1 with following formula:

$$f_i = 1 - \frac{C_i - C_{min}}{C_{max} - C_{min}}, \quad (12)$$

where C_i is carbon footprint of electricity source i , C_{min} is the energy source with lowest carbon footprint and C_{max} the source with the highest. I chose this approach for its simplicity and ease of implementation. Scaling the environmental impact of each energy source according to their relative magnitude of impact in comparison with other available energy sources is justified in my opinion, because sources with zero emissions over their life-cycle doesn't exist (and neither does sources with infinitely large impacts), so therefore the total power grid composition can only be as clean as the cleanest possible technology. Besides, the most carbon neutral technologies (Solar, wind and nuclear) are around the same order of magnitude in terms of carbon footprint. Conversely, the most carbon intensive sources (Coal, gas, and bioenergy) are also on the same order of magnitude, from the point of view of the carbon neutral technologies. The practical challenge for real-life implementation is the availability of real-time power generation data of the local power grid. I expect a macro scale implementation of this control strategy to work to reduce carbon footprint if the prerequisite of proper real-time data availability is met.

Additionally, I want to explore a hybrid control strategy, which I expect to achieve the best economic and environmental outcomes. The hybrid strategy combines *Nordpool* spot price -data with the *Energiategollisuus* energy source -data and it is of the form:

$$SP = SP_{max} + (SP_{min} - SP_{max}) * \left(1 - \frac{E_{pr} - E_{pr,min}}{E_{pr,max} - E_{pr,min}}\right) * (1 - E_f). \quad (13)$$

In the next chapter I intend to benchmark the economic and ecological outcomes of spot price –based strategy, electricity source composition –based strategy and the hybrid strategy.

7 RESULTS

7.1 MPC performance in refrigeration system

In figure 18, I performed a step response test with the MPC-controller in the simulator for freezer 1. I performed tests for up- and down shifting the freezer set-point temperature, because the dynamics of the system work differently to different control directions, and finally I switched measurement noise on to observe the performance of the controller when temperature measurement is degrading. The performance of the MPC is arguably optimal for set-point fidelity of freezer system. The control action in the event of lowering of the set-point from $-21,10\text{ }^{\circ}\text{C}$ to $-21,96\text{ }^{\circ}\text{C}$ results in fully opening the valve for at around 26 % opening, which ensures that the temperature follows set-point. Conversely, the raising of set-point from $-21,96\text{ }^{\circ}\text{C}$ back to $-20,67\text{ }^{\circ}\text{C}$ results in closing of the control valve, after which the control valve opening stabilises at around 18,5 % opening. The controller does not exhibit overshoot or steady-state deviations after reaching the set-point. When the system is in transient, the valve opening is either completely open in freezing event or completely closed, when temperature is lower than set-point, during most of the transient period. Therefore, the set-point fidelity with MPC is optimal and the system does not prove problematic to keep in control. Especially, when the controller set-point is decided based on *Nordpool* or *Energiateollisuus* data, the set-point changes happen hourly, so the control fidelity will not prove problematic. Strong measurement noise, as exhibited in the simulation in Figure 18, can offer the controller a bit more challenge. The system will not be kept in set-point temperature due to erratic feedback.

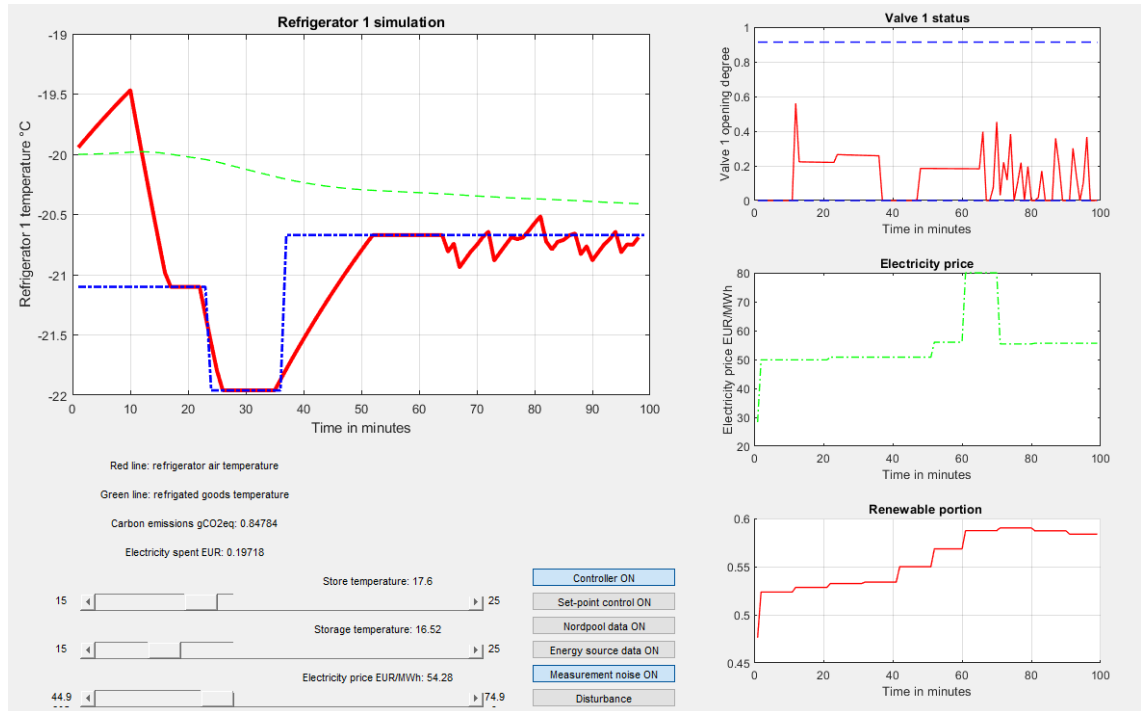


Figure 18. Step response the with freezer 1.

7.2 Control strategy benchmarks with simulations

I ran 4 simulations with different set-point control strategies in the Matlab simulator. I intend to compare the sums of power consumption costs and carbon emissions of all the refrigeration systems of the supermarket in different control strategies. These simulations are fixed set-point control strategy corresponding to conventional thermostat, energy spot price -based strategy, power grid composition -based strategy and a strategy that is affected by both, spot price and power grid composition. For the simulation sequence I used same data for all simulations, the January 2019 *Nordpool* spot price -data from Finland and January 2019 Finland's power grid composition obtained from *Energiategellisuus*. Because this data is from Finland on a January, the electricity spot price exhibits rather radical fluctuations, as night-time electricity prices occasionally skyrocket due to very cold nights.

As all conditions are the same for all simulations, except for the set-point selection strategy, I expect these simulations to allow me to compare the energy price and environmental impact of different control strategies in contrast to each other, The

expected outcome is of the comparison of simulations is that fixed set-point strategy is the most expensive and most carbon intensive. The spot price driven strategy I expect to be the cheapest, but it will not perform the best in terms of emissions. The power grid composition -based strategy I expect to be more expensive than spot price -based strategy, but I expect it to be cleanest. I expect the strategy based on both data sets to perform best overall. To keep the simulation time in reasonable boundaries for my computer to handle it, I limited the simulation steps to 400. Formula for calculating price of freezer power consumption over the data period is:

$$E_{price,total} = \sum_{i=400} \left(\sum(u_{k,i}) * E_{price,i} * \frac{P}{100000} \right), \quad (14)$$

where

$u_{k,i}$ =opening of valve k on time step i

E_{price} = Electricity spot price on step i

P =refrigerator power consumption (W/h)

Since I do not have information on the power consumptions of the refrigerator system, I made a guess that the maximum power consumption of each fully open control valve in all refrigerators is 100 Watts. I chose this value for simplicity and my understanding that it is in the vicinity of the correct order of magnitude for these values. Otherwise the term P would have to be replaced by a matrix that includes all the power consumptions values of all valves. Also, the base power consumptions of the refrigerators are not included in this calculation, but rather only the power consumed by the refrigeration action. Likewise, possible freezer power losses are assumed to not affect the current simulation for the sake of simplicity, however in real-life situation power losses could differentiate the results of similar test. My justification for these simplifications is this test is focused on DR aspects of refrigeration instead of energy efficiency.

7.2.1 Conventional Thermostat test results

The first simulation I ran is the fixed set-point selection strategy corresponding to a conventional thermostat. Figure 19 has the simulation trend for the runtime of the

simulation for freezer 1. At 400th simulation step, the cost of consumed electricity was 3,21 € and emissions caused by the consumed energy was equivalent to 0,73 grams of CO₂.

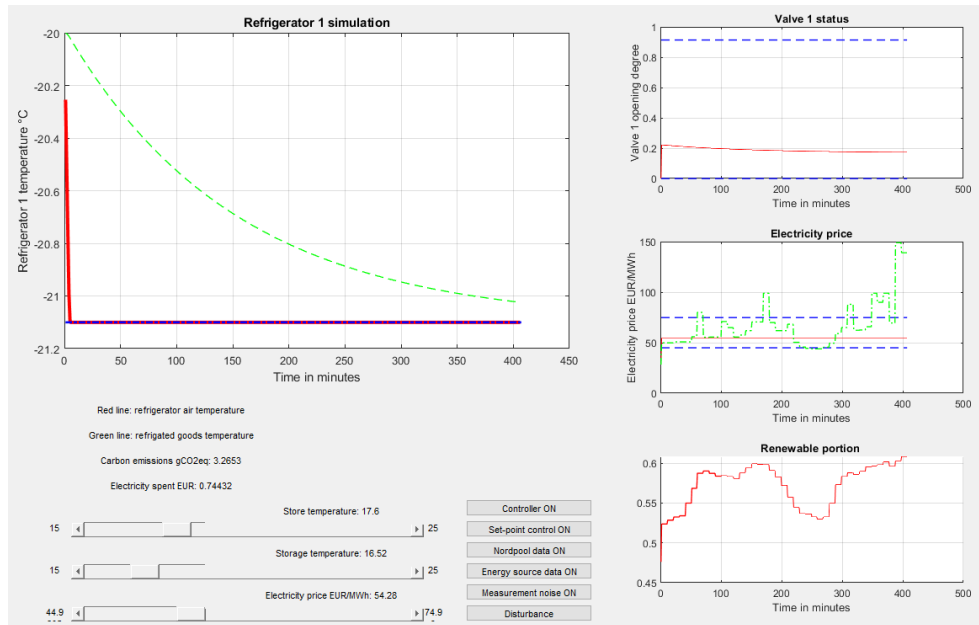


Figure 19. Simulation trend for conventional thermostat test.

The figure 20 has the trend for momentary emission caused by running the refrigerator system during the test and the figure 21 has the momentary electricity costs for the same period. As is expected, these trends are quite linear due to constant thermostat set-point.

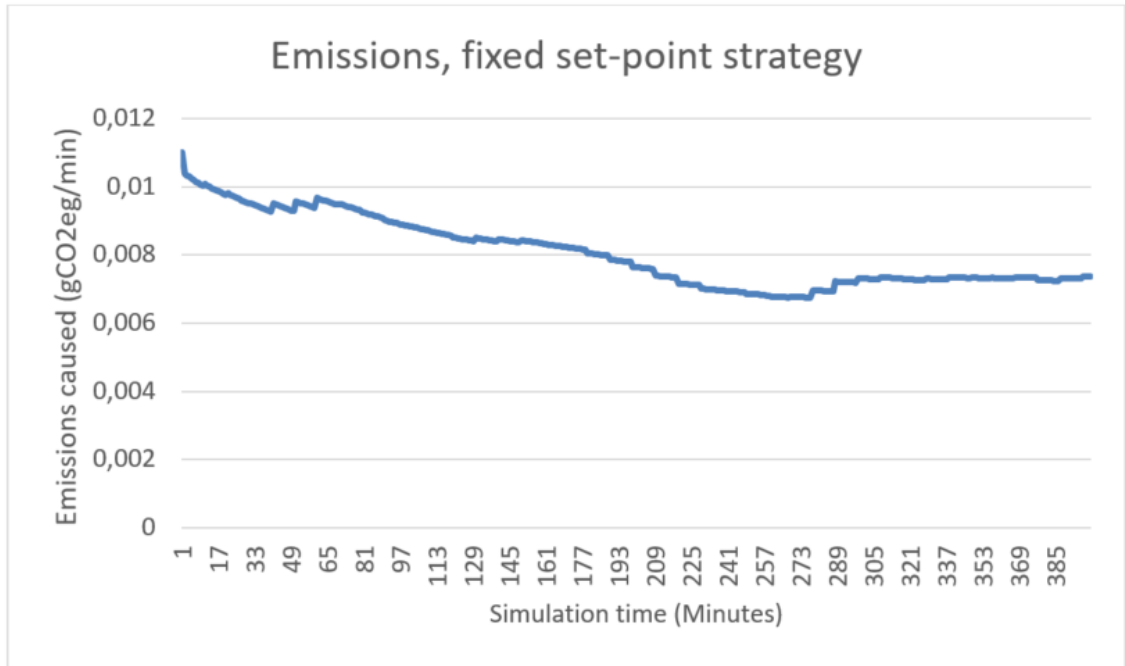


Figure 20. Momentary emissions caused by running the refrigerator system with conventional thermostat control strategy.

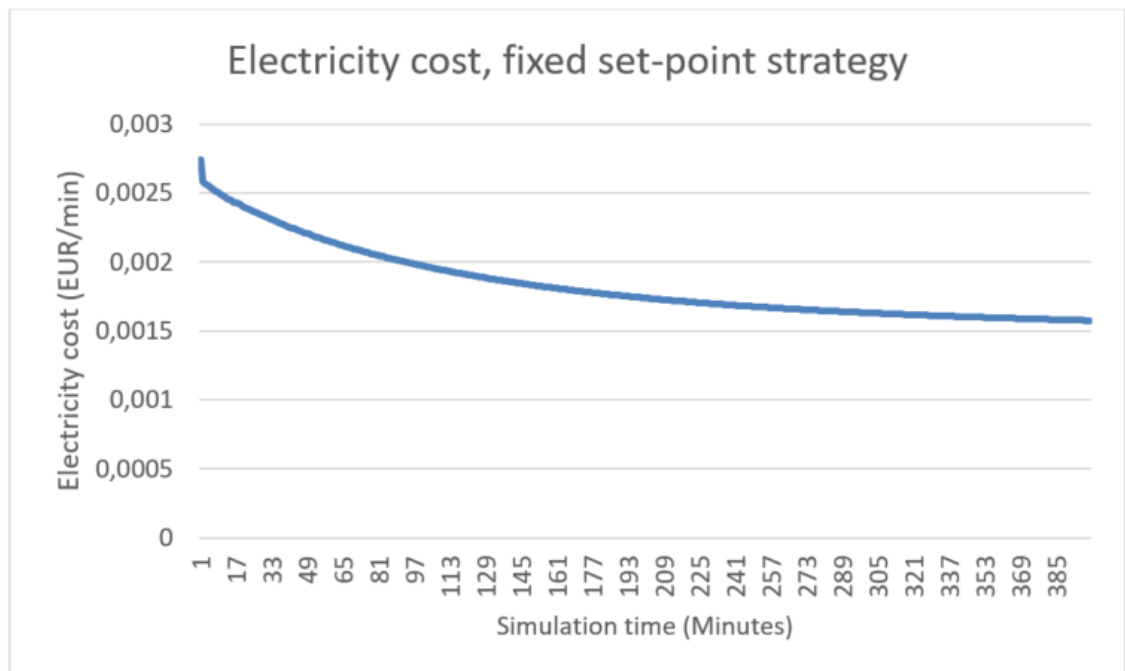


Figure 21. Momentary electricity cost of running the refrigerator system with conventional thermostat control strategy.

7.2.2 Nordpool data test results

The second simulation is the *Nordpool* spot price -based set-point selection strategy. Figure 21 has the simulation trend for the runtime of the simulation for freezer 1. At 400th simulation step, the cost of consumed electricity was 1,04 € and emissions caused by the consumed energy was equivalent to 0,252 grams of CO₂.

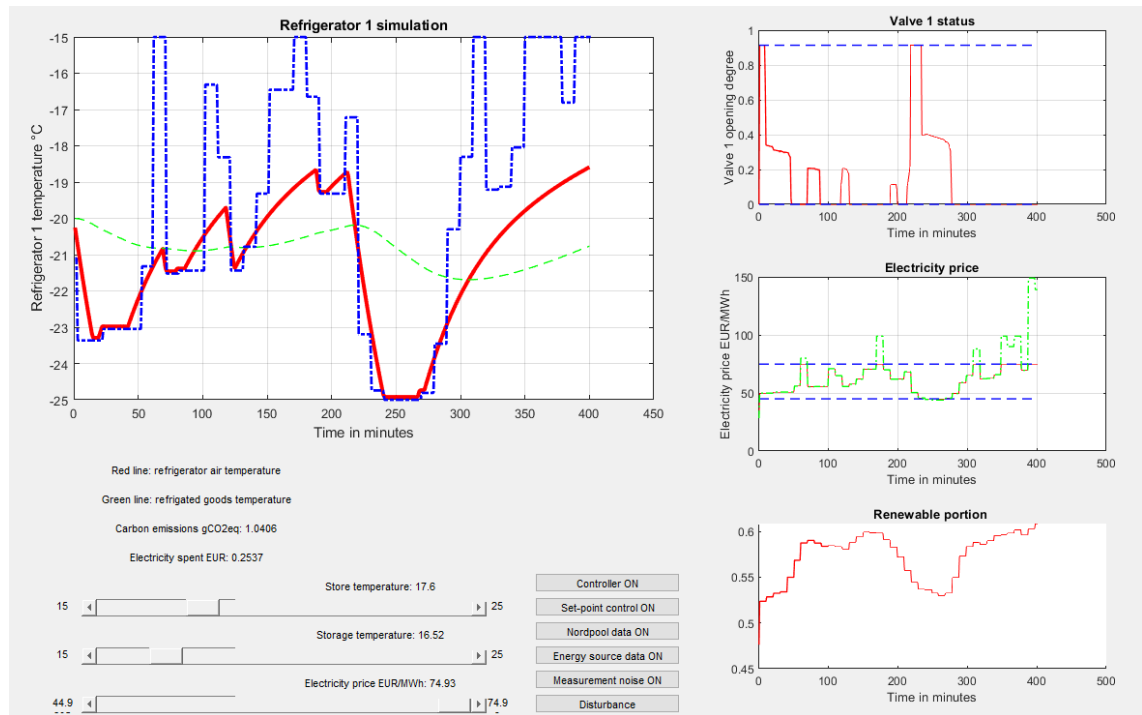


Figure 22. Simulation trend for *Nordpool* spot price data test.

The figure 23 has the trend for momentary emission caused by running the refrigerator system during the test and the figure 24 has the momentary electricity costs for the same period. Now we can see that these trends are shaped according to the spot price data. The trends do not completely match the freezer 1 valve action, because the refrigerators are not stopping their control actions after half point of the simulation, like the freezers do.

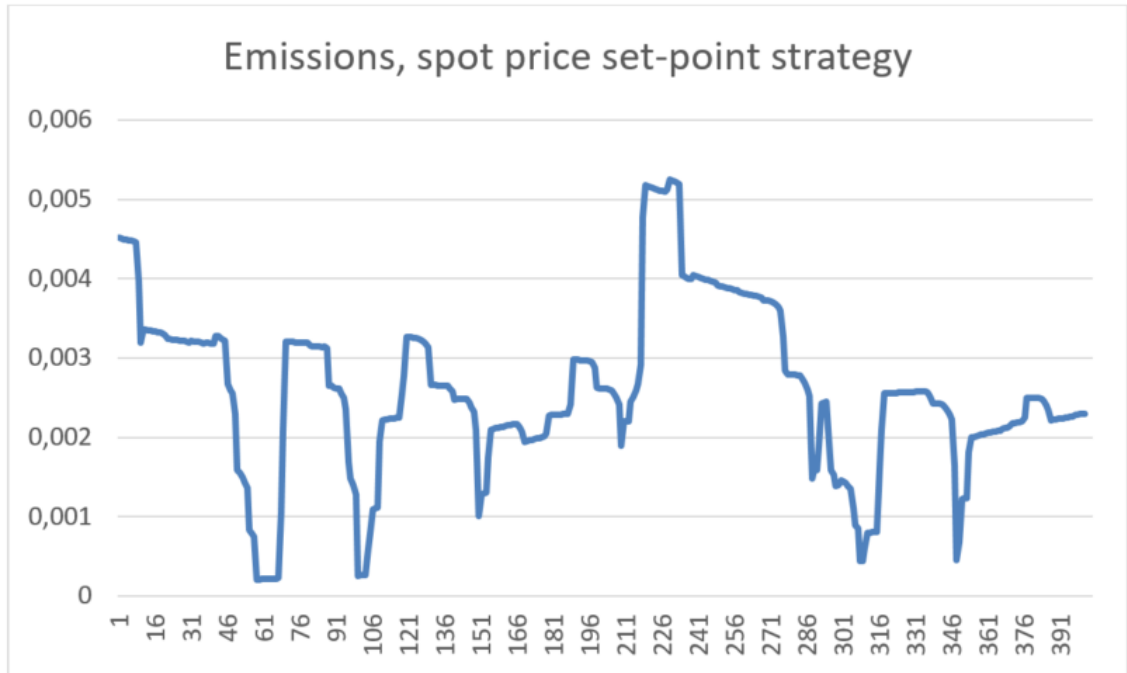


Figure 23. Momentary emissions caused by running the refrigerator system with *Nordpool* spot price control strategy.

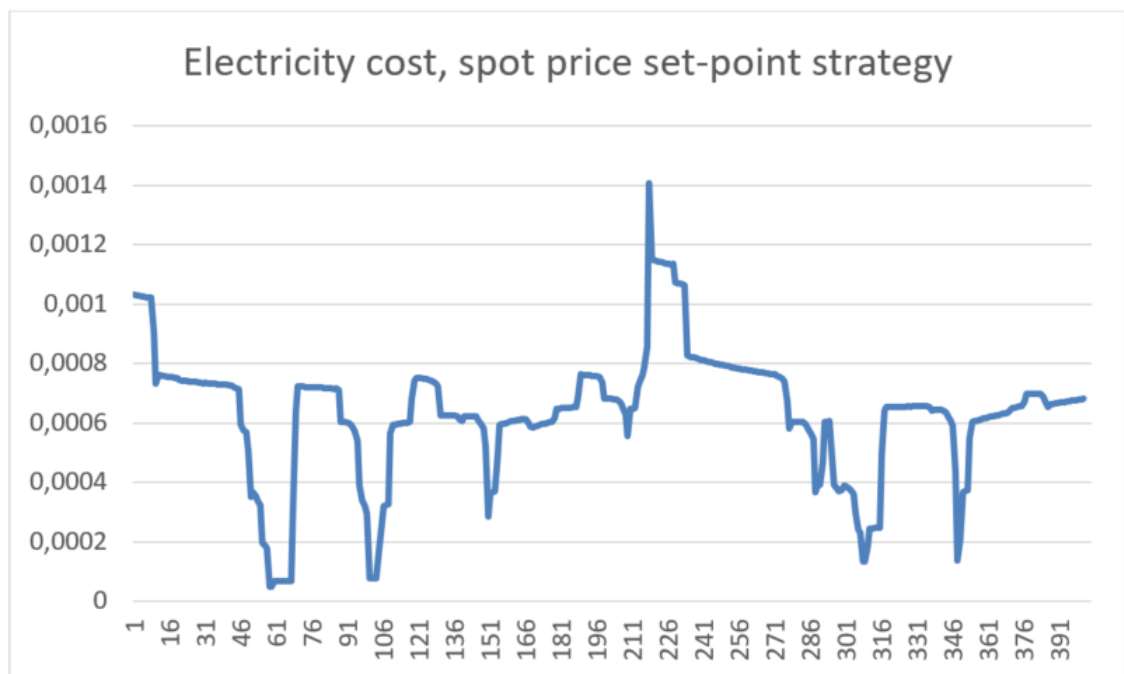


Figure 24. Momentary electricity cost of running the refrigerator system with *Nordpool* spot price control strategy.

7.2.3 Energy source data test results

The third simulation is the power grid composition -based set-point selection strategy. Figure 22 has the simulation trend for the runtime of the simulation for freezer 1. At 400th simulation step, the cost of consumed electricity was 1,11 € and emissions caused by the consumed energy was equivalent to 0,251 grams of CO₂.

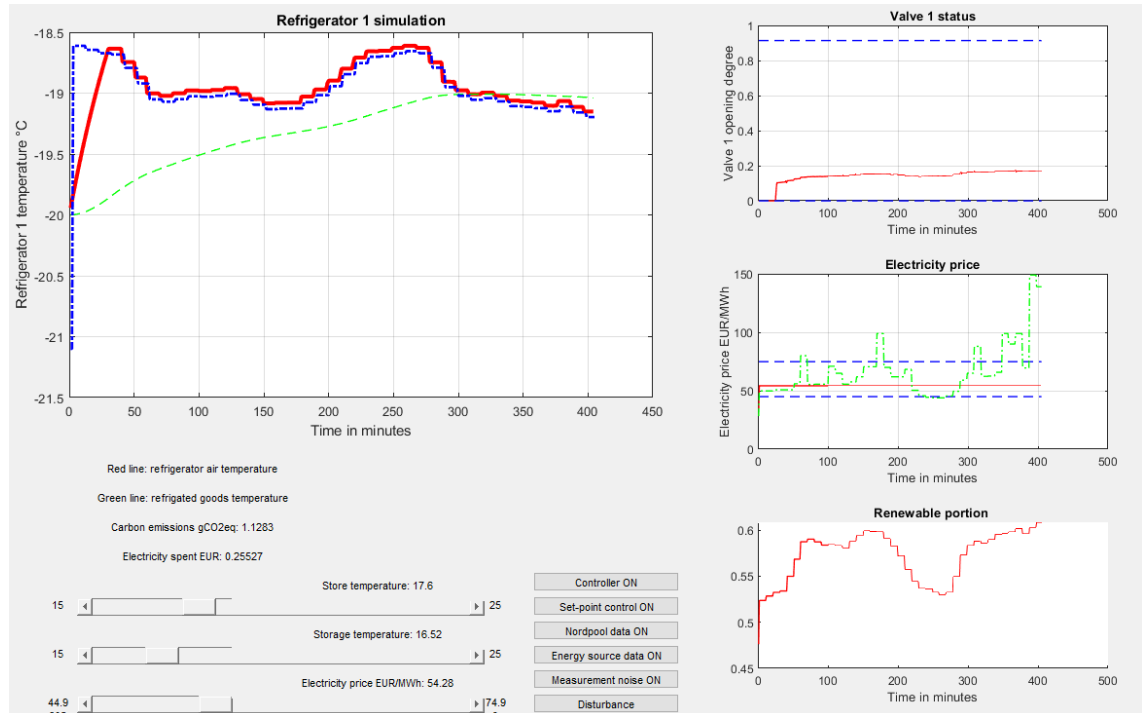


Figure 25. Simulation trend for power grid composition data test.

The figure 26 has the trend for momentary emission caused by running the refrigerator system during the test and the figure 27 has the momentary electricity costs for the same period. These trends have significantly less fluctuation than the spot price data trends. This is because the power grid composition has much less fluctuation during the simulation period. However, the shape of the renewable portion curve can be seen reflected into these curves.

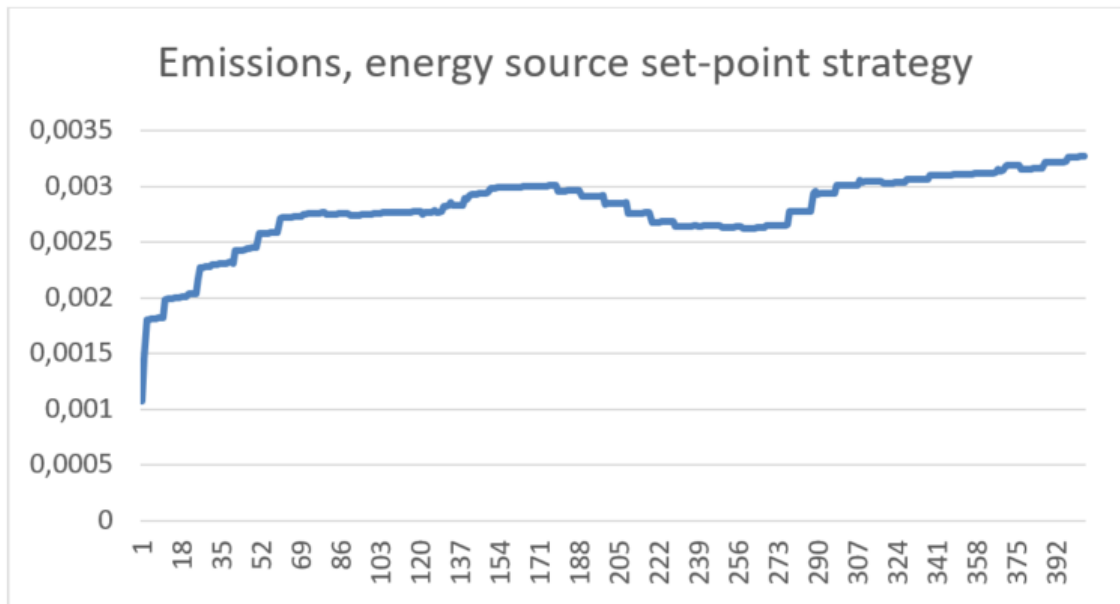


Figure 26. Momentary emissions caused by running the refrigerator system with energy source control strategy.

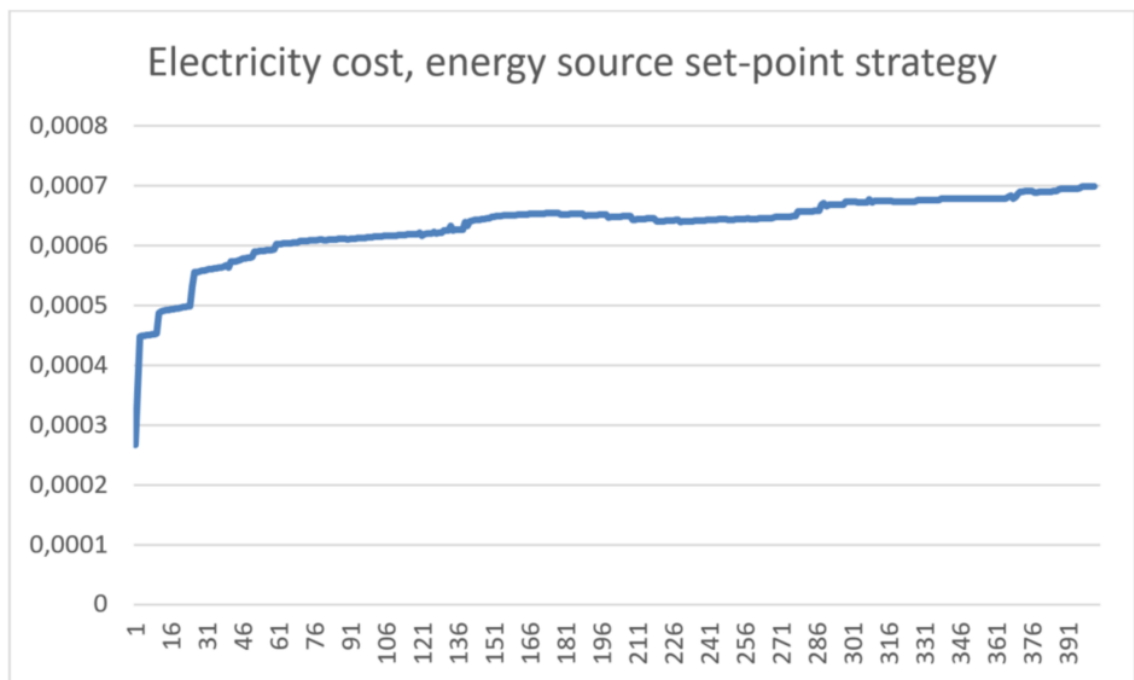


Figure 27. Momentary electricity cost of running the refrigerator system with energy source control strategy.

7.2.4 Nordpool data and energy source data test results

The fourth simulation control strategy combines the spot price data with power grid composition data to select the refrigerator temperature set-point. Figure 23 has the simulation trend for the runtime of the simulation for freezer 1. At 400th simulation step, the cost of consumed electricity was 0,969 € and emissions caused by the consumed energy was equivalent to 0,241 grams of CO₂.

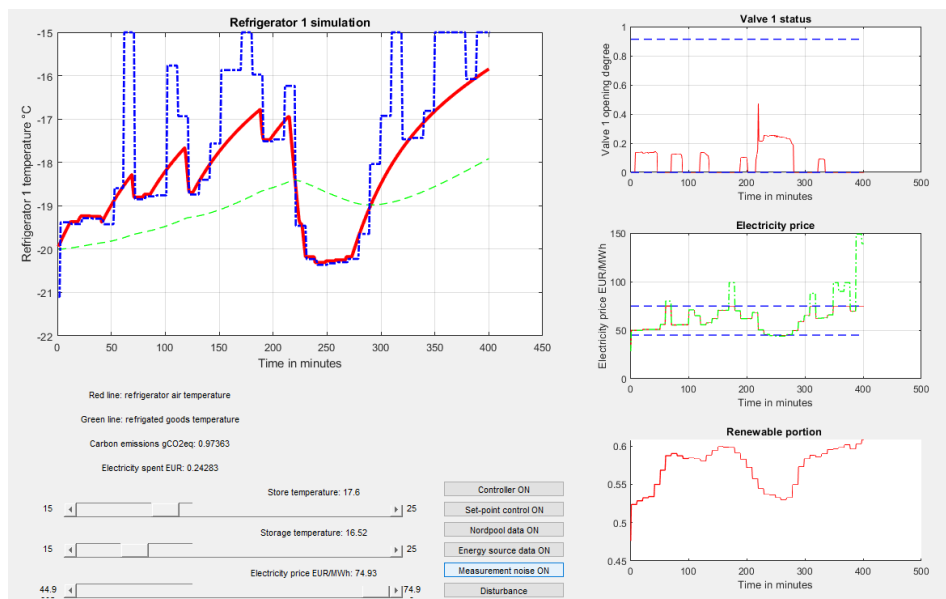


Figure 28. Simulation trend for *Nordpool*- and power grid composition data test.

The figure 29 has the trend for momentary emission caused by running the refrigerator system during the test and the figure 30 has the momentary electricity costs for the same period. The hybrid strategy trends have the spot price data fluctuations visible, but the combination with power grid composition data dampens the peaks of the fluctuation.

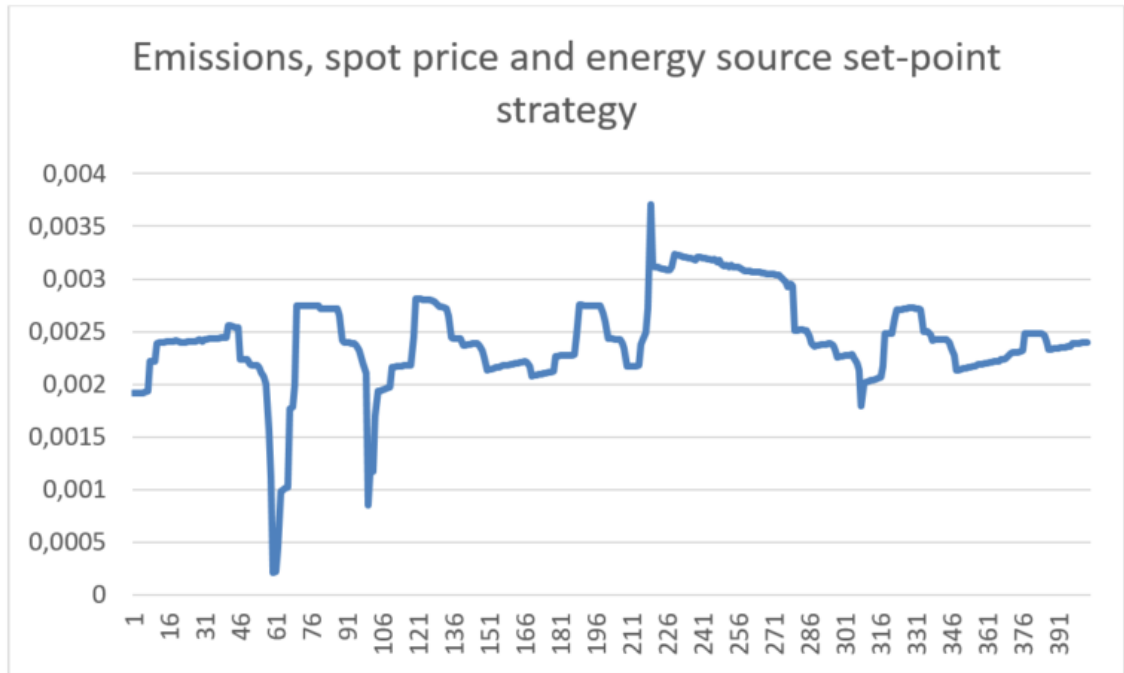


Figure 29. Momentary emissions caused by running the refrigerator system with hybrid control strategy.

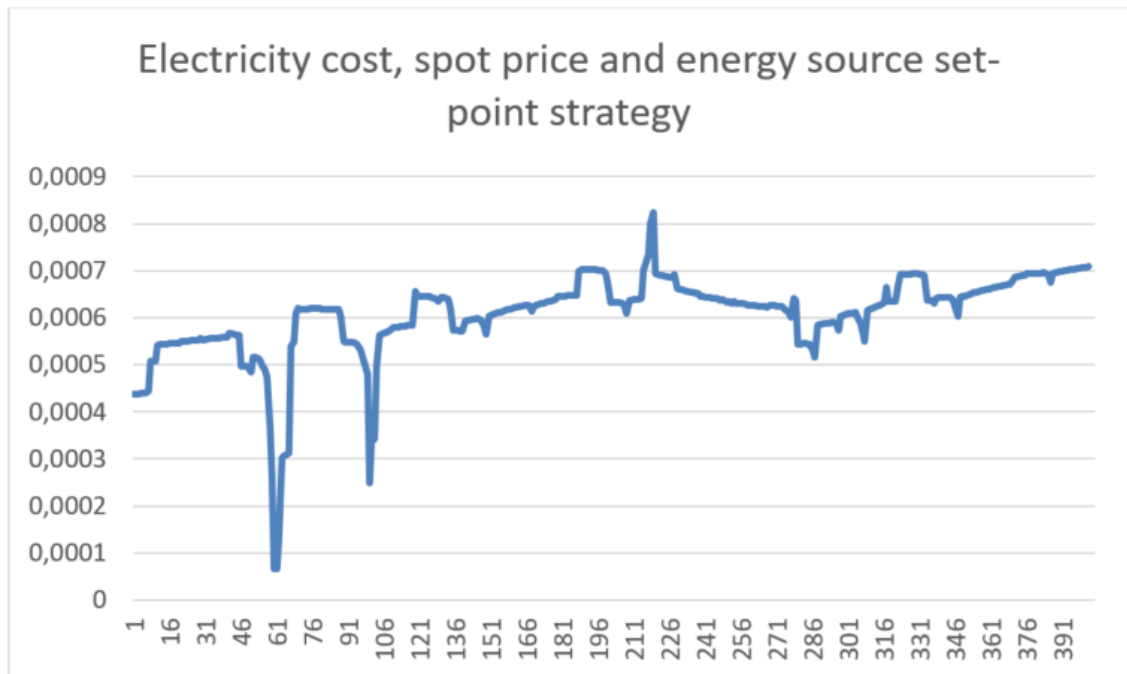


Figure 30. Momentary electricity cost of running the refrigerator system with hybrid control strategy.

7.2.5 Results breakdown

In Table 1. I have collected electricity costs and emissions cause by running the different control strategies for 400 simulation steps. A major take away here is, that any strategy outperforms conventional thermostat in both costs and emissions with the values being roughly one third in both aspects.

Table 1. Simulation results at simulation time step of 400 minutes.

	Cost of consumed electricity (EUR)	Emissions caused by consumed electricity (gCO ₂ eq),
Conventional thermostat	3,21	0,733
Spot price -based strategy	1,04	0,252
Power grid composition -based strategy	1,11	0,251
Spot price and Power grid composition -based strategy	0,969	0,241

A surprising take off the results is that the strategy combining spot price- and grid composition data yielded by far the best results in both, electricity price and carbon emissions. This could be explained by the fact, that a more restrained control strategy, like this one, will generally keep the temperature set-point higher, and therefore consume less energy.

The overall take away from these simulations in my opinion is, that control strategies that implement DR by utilizing refrigeration as a heat sink have good potential for cost and emission reduction. Especially in cold winter months, the DR strategies can prove to be very beneficial. Therefore, I find that further development in this area is warranted. The difference in emissions caused between spot price -based strategies and power grid composition -based strategies is surprisingly small. Therefore, utilizing the *Nordpool* spot price -data for DR purposes seems to be a promising strategy, since it does not require the acquisition of additional data about power grid composition. This means that, for the duration of the test data, the spot-price -data reflected the power grid composition well. However, longer simulations would be needed to verify, if the spot price -data could be universally utilized as a basis for DR, without increasing the emissions.

For these simulations I use the prediction horizon of 15 minutes, which allows the MPC-controller to see an upcoming set-point change up to 15 minutes ahead. The performance of the controller would vastly improve if the prediction horizon were much longer, either hours or even days. This would give the controller an ability to calculate an optimal control trajectory, which would capture the dynamics of the whole circadian rhythm and thus could unlock the whole DR potential of the controller. I use this value because it is manageable for my computer to perform the QP and a higher prediction horizon value would make the computation time too long. A workaround for this problem is to calculate an optimal set-point trajectory from spot-price- and power grid composition data, that I will discuss in chapter 8.2.

8 CONCLUSIONS

8.1 Lessons for S-Market Tuira control strategy

The Tuira S-Market power management adheres to micro-grid hierarchy, where each device, such as a refrigeration unit, follows orders dictated by the state of micro-grid itself. Micro-grid will make its own decisions according to amount of energy produced and consumed inside the micro-grid. Depending on the state of the grid, electricity spot price and possible aggregator demands, the micro-grid has four possible actions: procure energy from aggregator, sell energy to aggregator, store energy within the grid system or release energy from the system. Because of this, the shop-wide energy management algorithm requires higher level decision making than is presented in this thesis.

The lesson to take from research, such as (Laura M. Arciniegas, 2018), is that in order to maximize renewable energy utilization and in turn minimize fossil fuel consumption, all solar energy should be embedded within the power grid of the building. Therefore, the control algorithm of the building should direct the excess solar power is to be directed to power sinks once the solar power generation exceeds the building's base power consumption. Utilizing the solar power to over-freeze the heat sinks is always guaranteed to not include any fossil fuel -based power. However, the smart temperature set-point selection algorithm must have flexibility for special situations. If electricity price is low and renewable proportion of the power grid power generation is high, we can also lower the refrigeration set-point. Also, if the power grid is getting overloaded with unexpected power over-production, we must increase consumption by increasing refrigeration. On the contrary, when power grid has under generation, we minimize power consumption in our micro grid. Now we release the energy stored in the power sinks by closing the expansion valves of refrigerators and letting the temperature rise to a safe margin until we open them again. When power grid has low power generation, our micro grid releases generated solar power into the power grid to balance the power shortage.

In comparison to convenient control methods, controlling the refrigeration systems with MPC has the inherent advantage that constraints are built inside the controller itself by default. This results into automatic compliance with food safety limits and possible valve opening speed limitations. This means the that minimizing the system behaviour in terms

of cost function objective, be it minimum electricity price or minimum environmental impact, does not result in compromised safety even when operating close to system constraints. The *Nordpool* spot price -data driven approach could a part of the control algorithm, but the set-point temperature selection should consider the smart grid's own power generation and consumption in addition to the requirements and condition of the main power grid.

8.2 Further development

The DR aspect of the algorithm could be vastly enhanced by using data that is able to forecast further into the future than 15-minute prediction horizon I used in my simulations. Now, I would take advantage of the fact that weather- and electricity spot-price forecasts commonly have a 1-hour data resolution. Therefore, I would formulating a set-point optimizer, with the object of temperature set-point optimization according to hourly energy spot price data, energy source data, weather data or other relevant data concerning state of the power grid renewable portion. Here, a cost function formulation is required, the minimization of which would hourly compute a set-point trajectory for the next, for example, 100 hours, which is minimized to with the target of minimum electricity cost and environmental impact. The important requirement for the cost function formulation is that refrigerator system dynamics are included in the minimization. The desired outcome of the cost function minimization is a set-point trajectory that lowers the refrigerator system temperatures during periods of low priced clean-energy periods in order to prevent energy consumption during price peaks and/or dirty energy periods.

The Figure 31 illustrates a possible functional diagram for a controller hierarchy, where a set-point optimizer computes hourly an optimal set-point trajectory for the next 100 hours according to available data. The optimizer could utilize QP to minimize a cost function, which has the target of minimal electric costs and minimal caused emissions. The setpoint trajectory is fed to an MPC-controller, which works similarly as the one formulated in this thesis.

9 REFERENCES

- Aho, A. (2012). Computation and Computational Thinking. *The Computer Journal*. 55, 832-835.
- Balijepalli, V. &. (2011). *Review of demand response under smart grid paradigm*. 2011 IEEE PES International Conference on Innovative Smart Grid Technologies-India, ISGT India 2011. Noudettu osoitteesta
https://www.researchgate.net/publication/241635410_Review_of_demand_response_under_smart_grid_paradigm
- CAISO, C. I. (2016). Fast Facts: What the Duck Curve Tells us About Managing a Green Grid. California. Noudettu osoitteesta
https://www.caiso.com/Documents/FlexibleResourcesHelpRenewables_FastFacts.pdf
- Clayton Coleman, E. D. (2019). *Fossil Fuel Subsidies: A Closer Look at Tax Breaks and Societal Costs*. The Environmental and Energy Study Institute (EESI). Noudettu osoitteesta
https://www.eesi.org/files/FactSheet_Fossil_Fuel_Subsidies_0719.pdf
- D.Q. Mayne, J. R. (2000). Constrained model predictive control: Stability and optimality. *Automatica*, 789-814. Noudettu osoitteesta
<http://www.sciencedirect.com/science/article/pii/S0005109899002149>
- Danfoss. (2 2009). *Food Retail CO2 Refrigeration Systems*. Noudettu osoitteesta
http://files.danfoss.com/TechnicalInfo/Dila/01/DKRCEPAR1A102_The%20Food%20Retail%20CO2%20application%20handbook_DILA.pdf
- Denholm, P. a. (2015). *Overgeneration from solar energy in california. a field guide to the duck chart*. National Renewable Energy Lab.(NREL), Golden, CO (United States). Noudettu osoitteesta <https://www.nrel.gov/docs/fy16osti/65023.pdf>
- DietmarBartz, E. S. (2018). *Energy Atlas 2018: Figures and Facts about Renewables in Europe*. Noudettu osoitteesta <https://energytransition.org/2018/04/europe-must-choose-a-green-future/>
- Energiateollisuus. (3. 3 2020). *Sähkön tuntidata*. Noudettu osoitteesta Energiateollisuus:
https://energia.fi/uutishuone/materiaalipankki/sahkon_tuntidata.html#material-view
- ENERSON. (September 2015). *Commercial CO2 Refrigeration Systems*. Noudettu osoitteesta
[http://www.emersonclimate.com/Documents/FlowControls/pdf/2015CO2-07-R2-Commerical-CO2-Handbook-\(Sept2015\).pdf](http://www.emersonclimate.com/Documents/FlowControls/pdf/2015CO2-07-R2-Commerical-CO2-Handbook-(Sept2015).pdf)
- Eric S. Hittinger, I. M. (2015). *Bulk Energy Storage Increases United States Electricity System Emissions*. American Chemical Society. Noudettu osoitteesta
<https://pubs.acs.org/doi/full/10.1021/es505027p>
- Evans, C. L. (2009). *CO2 Unit Coolers for Supermarket Refrigeration System*. Bohn CO2 Unit Coolers,.
- Hovgaard, T. &. (2013). Nonconvex model predictive control for commercial refrigeration. *International Journal of Control*. Noudettu osoitteesta
https://www.researchgate.net/publication/262869975_Nonconvex_model_predictive_control_for_commercial_refrigeration

- Hovgaard, T. G. (2011). Power consumption in refrigeration systems - modeling for optimization. *4th International Symposium on Advanced Control of Industrial Processes*, 234-239.
- Hovgaard, T. G. (2012a). Model predictive control technologies for efficient and flexible power consumption in refrigeration systems. *Energy*, 105-116.
- Kim, W. &.b. (2010). Impact of carbon cost on wholesale electricity price: A note on price pass-through issues. *Energy*, 3441-3448. Noudettu osoitteesta https://www.researchgate.net/publication/222229365_Impact_of_carbon_cost_on_wholesale_electricity_price_A_note_on_price_pass-through_issues
- LaMonica, M. (29. April 2014). *greenbiz.com*. Noudettu osoitteesta GreenBiz 101: What do you need to know about demand response?: <https://www.greenbiz.com/article/greenbiz-101-what-do-you-need-know-about-demand-response>
- Laura M. Arciniegas, E. H. (2018). Tradeoffs between revenue and emissions in energy storage operation. *Energy*, 1-11. Noudettu osoitteesta <http://www.sciencedirect.com/science/article/pii/S0360544217318145>
- Lew, D. &.L. (2013). Wind and Solar Curtailment. London: 12th International Workshop on Large-Scale Integration of Wind Power into Power Systems as well as on Transmission Networks for Offshore Wind Power Plants. Noudettu osoitteesta https://www.researchgate.net/publication/259575369_Wind_and_Solar_Curtailment#:~:text=curtailment%20broadly%20to%20refer%20to,for%20curtailment%2C%20and%20system%20operators
- Liu, X. &. (2018). Economic model predictive control of boiler-turbine system. *Journal of Process Control*, 59-67.
- Lueken, R. &. (2014). The effects of bulk electricity storage on the PJM market. *Energy Systems*, 677-704.
- Mahesh Morjaria, E. -E. (4. 4 2019). *Flexible Solar Power: Unlocking Solar's Full Potential*. Noudettu osoitteesta <https://www.esig.energy/flexible-solar-power-unlocking-solars-full-potential/>
- Manfred Morari, J. H. (1999). Model predictive control: past, present and future. *Computers & Chemical Engineering*, 667-682. Noudettu osoitteesta <http://www.sciencedirect.com/science/article/pii/S0098135498003019>
- Marius Dillig, M. J. (2016). The impact of renewables on electricity prices in Germany – An estimation based on historic spot prices in the years 2011–2013,. *Renewable and Sustainable Energy Reviews*,, 7-15. Noudettu osoitteesta <http://www.sciencedirect.com/science/article/pii/S1364032115013866>
- Mercer, D. (30. 11 2019). *ABC News Australia*. Noudettu osoitteesta The rise of solar power is jeopardising the WA energy grid, and it's a lesson for all of Australia: <https://www.abc.net.au/news/2019-12-01/rise-of-rooftop-solar-power-jeopardising-wa-energy-grid/11731452>
- Nordpool. (26. 10 2019). *Regulating Power FI in EUR/MWh, MWh*. Noudettu osoitteesta <https://www.nordpoolgroup.com/>

- Pehl, M. A. (2017). Understanding future emissions from low-carbon power systems by integration of life-cycle assessment and integrated energy modelling. *Nat Energy* 2, 939–945. Noudettu osoitteesta <https://www.nature.com/articles/s41560-017-0032-9#citeas>
- Rivers, N. (2005). *Management of energy usage in a supermarket refrigeration systems*. The institute of Refrigeration.
- Rossiter, J. (2003). *Model-based Predictive Control-a Practical Approach*. Noudettu osoitteesta https://books.google.fi/books?id=owznQTI-NqUC&printsec=frontcover&source=gbs_atb#v=onepage&q=mimic&f=false
- Schneider, E. -N. (2009). *Demand Response Energy Solutions*. Noudettu osoitteesta <https://www.graybar.com/documents/schneider-demand-response.pdf>
- Shafiei, S. E. (2015). *Control Methods for Energy Management of Refrigeration Systems*. Department of Electronic Systems, Aalborg University.
- Tenhomaa, J. J. (2016). DEVELOPMENT OF A DYNAMIC MATHEMATICAL MODEL FOR DEMAND SIDE MANAGEMENT OF THE GROCERY STORE S-MARKET TUIRA. *Master's thesis, University of Oulu*.
- Tor Aksel N. Heirung, J. A. (2017). Stochastic model predictive control — how does it work?., *Computers & Chemical Engineering*,, 158-170. Noudettu osoitteesta (<http://www.sciencedirect.com/science/article/pii/S0098135417303812>)
- VTT, K. K. (2020). *S-Market Tuira Smartgrid*. Noudettu osoitteesta <http://smartgrid.vtt.fi/s-market/tuira/>